

A *Phytophthora capsici* RXLR Effector Targets and Inhibits a Plant PPlase to Suppress Endoplasmic Reticulum-Mediated Immunity

Guangjin Fan¹, Yang Yang², Tingting Li², Wenqin Lu¹, Yu Du³, Xiaoyu Qiang², Qujiang Wen¹ and Weixing Shan^{2,*}

¹State Key Laboratory of Crop Stress Biology for Arid Areas and College of Plant Protection, Northwest A&F University, Yangling, Shaanxi 712100, China

²State Key Laboratory of Crop Stress Biology for Arid Areas and College of Agronomy, Northwest A&F University, Yangling, Shaanxi 712100, China

³State Key Laboratory of Crop Stress Biology for Arid Areas and College of Horticulture, Northwest A&F University, Yangling, Shaanxi 712100, China

*Correspondence: Weixing Shan (wxshan@nwfau.edu.cn)

<https://doi.org/10.1016/j.molp.2018.05.009>

ABSTRACT

Phytophthora pathogens secrete a large arsenal of effectors that manipulate host processes to create an environment conducive to pathogen colonization. However, the underlying mechanisms by which *Phytophthora* effectors manipulate host plant cells still remain largely unclear. In this study, we report that PcAvr3a12, a *Phytophthora capsici* RXLR effector and a member of the Avr3a effector family, suppresses plant immunity by targeting and inhibiting host plant peptidyl-prolyl *cis-trans* isomerase (PPlase). Overexpression of PcAvr3a12 in *Arabidopsis thaliana* enhanced plant susceptibility to *P. capsici*. FKBP15-2, an endoplasmic reticulum (ER)-localized protein, was identified as a host target of PcAvr3a12 during early *P. capsici* infection. Analyses of *A. thaliana* T-DNA insertion mutant (*fkbp15-2*), RNAi, and overexpression lines consistently showed that FKBP15-2 positively regulates plant immunity in response to *Phytophthora* infection. FKBP15-2 possesses PPlase activity essential for its contribution to immunity but is directly suppressed by PcAvr3a12. Interestingly, we found that FKBP15-2 is involved in ER stress sensing and is required for ER stress-mediated plant immunity. Taken together, these results suggest that *P. capsici* deploys an RXLR effector, PcAvr3a12, to facilitate infection by targeting and suppressing a novel ER-localized PPlase, FKBP15-2, which is required for ER stress-mediated plant immunity.

Key words: RXLR effector, Avr3a, FKBP, ER stress, immunity, *Phytophthora capsici*

Fan G., Yang Y., Li T., Lu W., Du Y., Qiang X., Wen Q., and Shan W. (2018). A *Phytophthora capsici* RXLR Effector Targets and Inhibits a Plant PPlase to Suppress Endoplasmic Reticulum-Mediated Immunity. *Mol. Plant.* **11**, 1067–1083.

INTRODUCTION

Plants have evolved multiple complex signal transduction pathways that synergistically respond to pathogen threats. These responses are conferred by a two-layered innate immune system, consisting of pattern-triggered immunity (PTI) and effector-triggered immunity (Jones and Dangl, 2006; Dodds and Rathjen, 2010). These innate immune systems often rely on basic cellular processes to defend against pathogens, such as the endoplasmic reticulum (ER) quality control system (Li et al., 2009) and hormone signaling (Kazan and Lyons, 2014). However, successful plant pathogens can secrete a plethora of effectors that interfere with many host cellular processes in order to establish colonization (Dou and Zhou, 2012; Qiao et al., 2013; Turnbull et al., 2017). Thus, insights into effector targets and target functions reveal both pathogen infection mechanisms and novel plant components of immunity.

Secreted and transmembrane proteins are translocated into the ER and are properly folded and modified through a sophisticated ER quality control (ER-QC) system to guarantee their functionality before being transported to their final destination (Liu and Howell, 2010). Under abiotic or biotic stress, unfolded or misfolded proteins often accumulate in the ER lumen, which results in ER stress. To relieve ER stress and restore ER homeostasis, ER membrane-localized stress sensors such as the transcription factor bZIP28 subsequently activate the unfolded protein response (UPR) (Howell, 2013). The UPR includes the induction of ER chaperones and foldases, such as heat-shock proteins (HSPs), protein disulfide isomerases, and peptidyl-prolyl *cis-trans* isomerases (PPIases) (Braakman

and Hebert, 2013), that enhance protein folding in the ER. In addition, the efficiency of protein translation is attenuated, global gene expression is inhibited, the capacity of protein secretion is potentiated, and ER-associated protein degradation is induced in order to restore ER homeostasis and, hence, functionality (Liu and Howell, 2010). In plants, there are at least two UPR pathways, which are mediated by IRE1-bZIP60 and bZIP28, respectively (Körner et al., 2015). Increasing evidence suggests that adapting ER folding capacity and UPR regulation plays an important role in plant immunity. For example, the pattern-recognition receptor EFR requires the ER-QC complex SDF2-ERdj3B-BiP for proper processing (Nekrasov et al., 2009), and the secretion of *Arabidopsis thaliana* pathogenesis-related proteins requires HSP AtBiP2 (Wang et al., 2005). Furthermore, the IRE1-bZIP60 branch of UPR is crucial for inducing systemic acquired resistance (SAR) against bacterial pathogens and abiotic stress tolerance (Moreno et al., 2012). Interestingly, in rice the underlying SAR-mediated priming effect depends on *WRKY33*, a gene that is well-known to be involved in salicylic acid (SA)-mediated defense in *A. thaliana* (Wakasa et al., 2014). In addition to supporting the production of plant immunity components, ER stress can trigger cell death, which can be part of an effective immune response, but can be also deployed by some microbes to establish colonization (Qiang et al., 2012; Jing et al., 2016). Taken together, the ER has a significant effect on the outcome of plant-pathogen interactions. However, the molecular mechanisms of how ER-associated or -regulated processes participate in plant immunity during plant-pathogen interactions are not well understood.

Plant pathogenic oomycetes, such as *Phytophthora infestans*, *Phytophthora sojae*, and *Phytophthora capsici*, cause many destructive crop diseases (Kamoun et al., 2015). They secrete a large number of effectors to facilitate plant infection. The first oomycete avirulence effector gene *Avr1b* was obtained by map-based cloning (Shan et al., 2004). Based on the sequences of cloned avirulence effectors, a conserved N-terminal Arg-x-Leu-Arg (RXLR) motif was identified (Rehmany et al., 2005). This motif plays an important role in enabling delivery of effectors into host plant cells (Whisson et al., 2007; Dou et al., 2008; Kale et al., 2010; Wawra et al., 2017). Taking advantage of genome sequencing, hundreds of putative RXLR effector genes have been predicted in each sequenced *Phytophthora* genome (Tyler et al., 2006; Haas et al., 2009; Lamour et al., 2012). Their functions and underlying mechanisms of these effectors have become a central focus of plant resistance and immunity research. Oomycete RXLR effectors have been shown to both directly hijack plant resistance pathways (McLellan et al., 2013; King et al., 2014; Du et al., 2015) and utilize plant susceptibility factors (Wang et al., 2015; Boevink et al., 2016; Yang et al., 2016). Interestingly, several RXLR effectors were found to indirectly modulate plant immunity by interfering with general host cellular processes, including ER stress-mediated cell death (Jing et al., 2016), autophagosome formation (Dagdas et al., 2016), and RNA silencing (Qiao et al., 2013, 2015).

RXLR effectors are known to be highly diverse, and effector sequences rarely overlap with each other across a genus (Jiang et al., 2008). However, the Avr3a effector family represents an

exception with various homologs in at least three different *Phytophthora* species, i.e., *P. infestans*, *P. sojae*, and *P. capsici* (Bos, 2007), implying that this family has an important role in *Phytophthora* pathogenicity. *P. sojae* and *P. infestans* have relatively narrow host ranges and contain only a few copies of Avr3a-like effectors. In contrast, *P. capsici* infects a broad range of hosts including 45 species of cultivated plants (Hausbeck and Lamour, 2004), and there are at least 13 genes homologous to Avr3a in this species (*PcAvr3a1* to *PcAvr3a13*) (Bos, 2007). It was reported that *P. infestans* effector PiAvr3a suppresses INF1-triggered cell death by stabilizing CMPG1 (Bos et al., 2010) and inhibits PTI by associating with DRP2 (Chaparro-Garcia et al., 2015). PsAvr1b, an Avr3a homolog from *P. sojae*, suppresses BAX-triggered cell death (Dou et al., 2008). However, all 13 Avr3a homologs from *P. capsici* were neither recognized by potato resistance protein R3a nor able to suppress INF1-triggered cell death (Bos, 2007), implying that they have more specialized roles in *P. capsici* pathogenicity (Vega-Arreguin et al., 2014). To date, our understanding of the pathogenicity of *P. capsici* and the role of its effectors, including these PcAvr3a homologs, remains elusive.

We previously reported that *P. capsici* is a pathogen of *A. thaliana*, making it a model oomycete pathosystem (Wang et al., 2013). In this study, we show that *P. capsici* employs the effector PcAvr3a12 as an efficient suppressor of immune response to successfully colonize *A. thaliana*. Our analyses revealed that the ER-localized FKBP15-2 protein, a PPIase, is a direct target of this effector. We show that FKBP15-2 functions in the regulation of ER stress and plant immunity and demonstrate how its PPIase activity is modified by PcAvr3a12.

RESULTS

Overexpression of PcAvr3a12 Enhances Plant Susceptibility to *P. capsici* in *Arabidopsis*

Consistent with a previous study (Bos, 2007), our experiments showed that PcAvr3a12 could neither be recognized by resistance protein R3a nor suppress INF1-triggered cell death (Supplemental Figure 1) as reported for the well-studied *P. infestans* effector PiAvr3a, the closest homolog to PcAvr3a12 in *P. capsici*. Using *A. thaliana* as a model host of *P. capsici* (Wang et al., 2013), we infected the susceptible ecotype Columbia-0 (Col-0) with the PcAvr3a12-expressing *P. capsici* strain LT263. Real-time RT-PCR assays showed that PcAvr3a12 was upregulated during the early stages of infection, with a maximal expression level at 6 h post inoculation (hpi) (Figure 1A). To examine the role of PcAvr3a12 in *P. capsici* pathogenicity, we generated and characterized *A. thaliana* Col-0 transgenic lines expressing FLAG-PcAvr3a12 (Figure 1D). Leaves of FLAG-PcAvr3a12-expressing lines showed larger water-soaked lesions than the FLAG-GFP-expressing control line, when inoculated with *P. capsici* zoospore suspensions (Figure 1B). RT-PCR analyses were performed (Llorente et al., 2010; Pan et al., 2016) to determine the *P. capsici* biomass in these infected leaf areas. Consistent with lesion size, *P. capsici* biomass was more abundant on FLAG-PcAvr3a12-expressing lines than on the FLAG-GFP-expressing control lines (Figure 1C). These data indicate that PcAvr3a12 enhances the susceptibility of *A. thaliana* plants to *P. capsici*

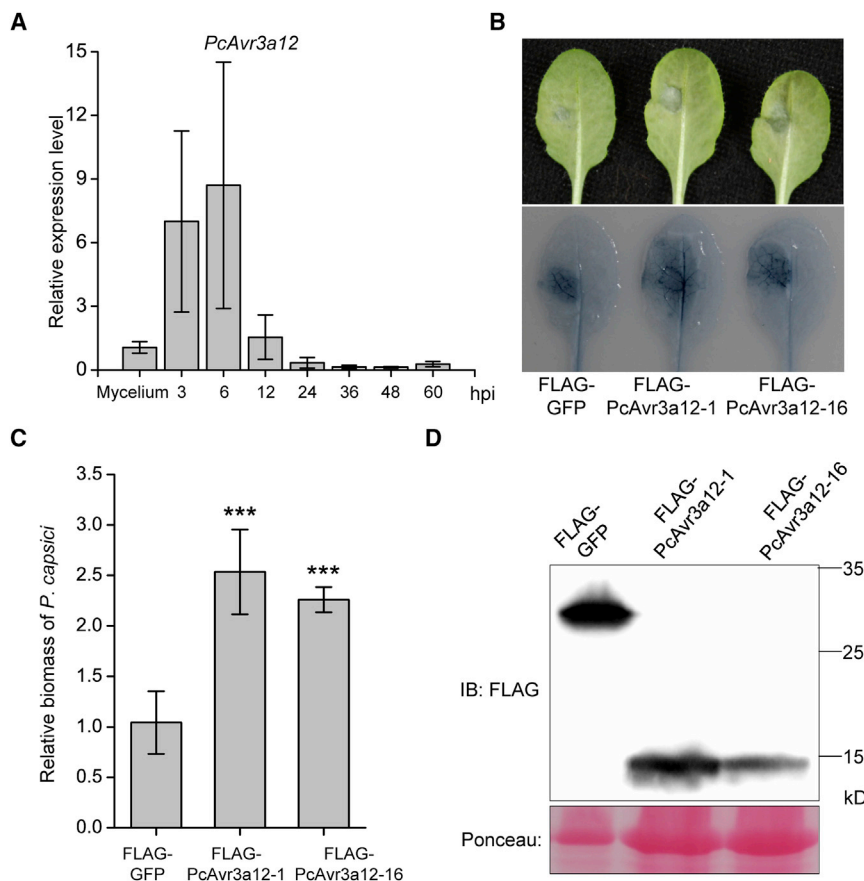


Figure 1. *P. capsici* RXLR Effector *PcAvr3a12* Is a Virulence Factor.

(A) Expression of *PcAvr3a12* at different stages of infection was determined by qRT-PCR. Four-week-old leaves from *A. thaliana* Col-0 were inoculated with *P. capsici* zoospores. Total RNA was extracted from mycelia and infected leaves at 3, 6, 12, 24, 36, 48, and 60 h post inoculation (hpi). The *P. capsici* actin gene (gene ID: gj|Phyca11|132086) was used as an internal control. Error bars indicate SD of three biological replicates.

(B) Transgenic *A. thaliana* lines constitutively expressing FLAG-*PcAvr3a12* showed enhanced susceptibility to *P. capsici* infection. Image was taken at 60 hpi.

(C) The degree of *P. capsici* colonization at 60 hpi was determined by qRT-PCR. Primers specific for the *P. capsici* actin gene and the *A. thaliana* *UBC9* gene (gene ID: AT4G27960) were used. Error bars indicate SD of four biological replicates, with at least eight leaves per replicate. Asterisks indicate significant differences (***) $P < 0.01$.

(D) Immunoblotting (IB) using anti-FLAG antibody to detect effector protein expression. Two independent transgenic *A. thaliana* lines expressing FLAG-*PcAvr3a12* and one FLAG-GFP-expressing *A. thaliana* line were examined.

infection when overproduced in plant cells, and thus might function as a virulence factor.

PcAvr3a12 Physically Interacts with a Host Protein, FKBP15-2

To investigate how *PcAvr3a12* attenuates *A. thaliana* resistance against *P. capsici*, we screened a yeast two-hybrid (Y2H) library created from *Phytophthora parasitica*-infected *A. thaliana* cDNA for *PcAvr3a12*-interacting proteins. This led to the identification of AtFKBP15-2 as a potential target of *PcAvr3a12*. AtFKBP15-2 contains an N-terminal secretion signal, an FKBP (FK506-binding protein) domain, and a C-terminal ER retention signal (Figure 2B) (He et al., 2004). Additional Y2H assays were performed to validate the interaction between *PcAvr3a12* and AtFKBP15-2. PiAvr3a^{K1}, *PcAvr3a14* (a PiAvr3a homolog cloned from *P. capsici* LT263; Supplemental Figure 2A), AtFKBP15-1 (the closest homolog of AtFKBP15-2 in *A. thaliana*; Figure 2B and Supplemental Figure 2B), PcFKBP35 (the best Blast hit of AtFKBP15-2 in *P. capsici*; Supplemental Figure 2B), and the respective empty vectors were used as controls in these Y2H assays. Yeast strain AH109 co-expressing AtFKBP15-2 (the secretion signal peptide [SP] and ER retention signal of FKBP15-2 were deleted) and *PcAvr3a12* grew on selective medium and yielded α -galactosidase activity, whereas all controls did not (Figure 2A), confirming the specific interaction between FKBP15-2 and *PcAvr3a12* in yeast. Additionally, exchanges of AtFKBP15-2 and *PcAvr3a12* between the prey plasmid (AD) and bait plasmid (BD) further confirmed this interaction even under conditions with higher selection pressure (Figure 2C).

To further validate whether this interaction can occur *in planta*, we carried out co-immunoprecipitation (CoIP) assays. The p35S::7*myc-*PcAvr3a12* construct was co-transformed with either p35S::SP-GFP-FKBP15-2-NDEL (GFP was fused with FKBP15-2 downstream of its SP), p35S::FLAG-GFP, or the empty vector in *Nicotiana benthamiana* leaves through agroinfiltration. Total proteins were extracted from infiltrated leaves and were immunoprecipitated with GFP-Trap agarose beads. Immunoblotting experiments showed that, although 7*myc-*PcAvr3a12* was equally expressed in all leaves, it was co-immunoprecipitated in SP-GFP-FKBP15-2-NDEL-expressing samples, but not in the FLAG-GFP or empty vector samples (Figure 2D and Supplemental Figure 3A). In similar experiments, FLAG-IP assays also showed that SP-directed GFP-FKBP15-2-NDEL was enriched with FLAG-*PcAvr3a12*, but not with FLAG-PiAvr3a^{K1}, although all proteins were detected in the input fractions (Supplemental Figure 3B and 3C). These results indicate that *PcAvr3a12* associates with FKBP15-2 *in planta*.

Expression of FKBP15-2 Is Upregulated at the Early Stages of *Phytophthora* Infection

To characterize the expression pattern of FKBP15-2 during *P. capsici* infection, we measured its relative transcription levels at 0, 3, 6, 12, 24, 36, 48, and 60 hpi by RT-PCR. As observed for *PcAvr3a12* (Figure 1A), FKBP15-2 was upregulated in Col-0 during the early stages of *P. capsici* LT263 infection, reaching the highest expression level at 6 hpi (Figure 3A). Consistent with this, FKBP15-2 transcripts were also upregulated at early infection stages in *A. thaliana* (Col-0) roots inoculated with *P. parasitica* Pp016 zoospores (Figure 3B).

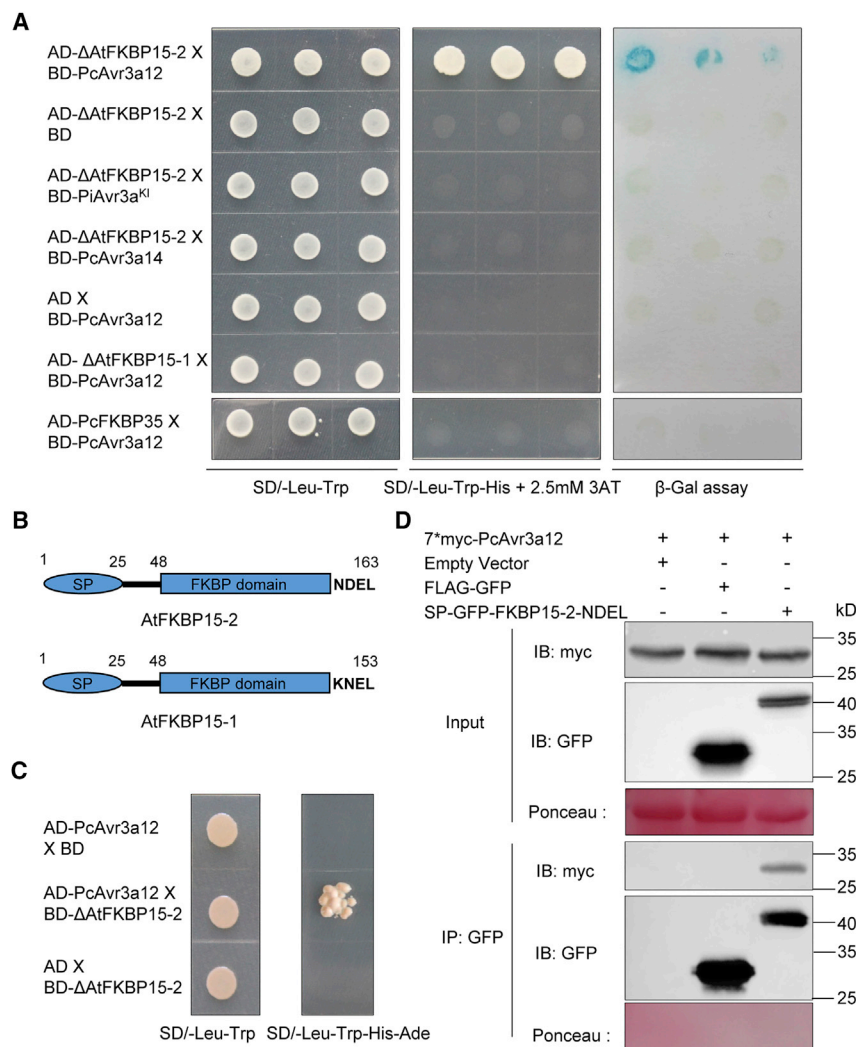


Figure 2. Identification of the Host Protein AtFKBP15-2 Interaction with *P. capsici* RXLR Effector PcAvr3a12.

(A) Y2H assays showing that PcAvr3a12 specifically interacts with AtFKBP15-2. Approximately 10^5 cells of yeast strain AH109 co-expressing the empty bait vector (BD) or a bait vector containing PcAvr3a12, PiAvr3a^{KI}, or PcAvr3a14 and the empty prey vector (AD) or a prey vector containing AtFKBP15-2, AtFKBP15-1, or PcFKBP35 were grown on auxotrophic media (SD/-Leu-Trp) (left panel). Only yeast cells co-expressing PcAvr3a12 and AtFKBP15-2 grew on auxotrophic media (SD/-Leu-Trp-His) and yielded β -galactosidase (β -Gal) activity (right panel). Δ AtFKBP15-2 and Δ AtFKBP15-1 represent specific protein constructs in which the SP and the potential ER retention signal, respectively, were deleted. Three independent experiments showed consistent results.

(B) Domain architectures of AtFKBP15-2 and AtFKBP15-1.

(C) The bait/prey swap experiments in Y2H assays confirmed that PcAvr3a12 specifically interacts with AtFKBP15-2. Yeast cells co-expressing PcAvr3a12 and FKBP15-2 grew on auxotrophic media (SD/-Leu-Trp-His-Ade), whereas the control pairs did not. Three independent experiments showed consistent results.

(D) Co-immunoprecipitation assays showing that PcAvr3a12 interacts with AtFKBP15-2 *in planta*. Total native protein extracts (Input) from agroinfiltrated leaves expressing the indicated proteins were precipitated with GFP-Trap agarose beads (IP: GFP), separated on SDS-PAGE gels, and blotted with specific antibodies. For the input fraction a similar amount of 7*myc-PcAvr3a12 and SP-GFP-FKBP15-2 was used. In immunoprecipitation fractions, 7*myc-PcAvr3a12 was detected in a complex with SP-GFP-FKBP15-2-NDEL but not with FLAG-GFP, and no 7*myc-PcAvr3a12 was detected in the immunoprecipitate from the empty vector sample. Protein size markers are indicated in kDa, and protein loading is indicated by Ponceau staining. The experiments were repeated twice with similar results.

GFP, and no 7*myc-PcAvr3a12 was detected in the immunoprecipitate from the empty vector sample. Protein size markers are indicated in kDa, and protein loading is indicated by Ponceau staining. The experiments were repeated twice with similar results.

To further characterize the expression profile of *FKBP15-2*, we cloned a 1097-bp promoter fragment of *FKBP15-2* (−1097 to −1 bp) from genomic DNA to drive the expression of the *GUS* gene. This promoter was predicted using the online bioinformatics tool Arabidopsis *cis*-regulatory element database (<http://arabidopsis.med.ohio-state.edu/AtcisDB>). Stable transgenic *A. thaliana* (Col-0) lines carrying the reporter construct pFKBP15-2::GUS were generated, and histochemical staining of these lines showed that GUS was activated by pFKBP15-2 in the majority of organs, although to various degrees, during all growth stages (Supplemental Figure 4).

FKBP15-2 Is Required for Plant Resistance to *Phytophthora*

To investigate the function of *FKBP15-2* in *Phytophthora* infection, we analyzed the T-DNA mutant line *fkbp15-2* (Col-0 background) carrying a T-DNA insertion in the second intron (Supplemental Figure 5A and 5B). The mutant showed similar growth phenotypes compared with Col-0 (Supplemental Figure 5C and

5D) despite a 98% reduction in *FKBP15-2* transcript (Figure 3C). Detached leaves of Col-0 and *fkbp15-2* plants were drop-inoculated with *P. capsici* zoospores. The infection lesions on mutant *fkbp15-2* were larger than those on Col-0 (Figure 3D), and we observed more pathogen colonization (Figure 3E). Similarly, *fkbp15-2* leaves showed larger lesions (Figure 3F) and more pathogen biomass (Figure 3G) when infected with *P. parasitica* Pp016, suggesting that *FKBP15-2* is required for plant resistance against both *Phytophthora* spp. In support of this conclusion, analyses of *FKBP15-2*-overexpressing and -silenced *A. thaliana* transformants (Supplemental Figure 5E) revealed significant changes in *P. capsici* colonization (Figure 3H). Considering that *P. parasitica* and *P. capsici* are two common soil-borne pathogens, with the former being less aggressive on Col-0, the roots of 2-week-old *fkbp15-2* and Col-0 seedlings were dip-inoculated with *P. parasitica* zoospores. As expected, the pathogen biomass in *fkbp15-2* roots was higher than that in Col-0 (Figure 3I). Furthermore, expression of marker genes of SA and jasmonic acid (JA) pathways, *PR1* and *PDF1.2*, respectively (Uknes et al.,

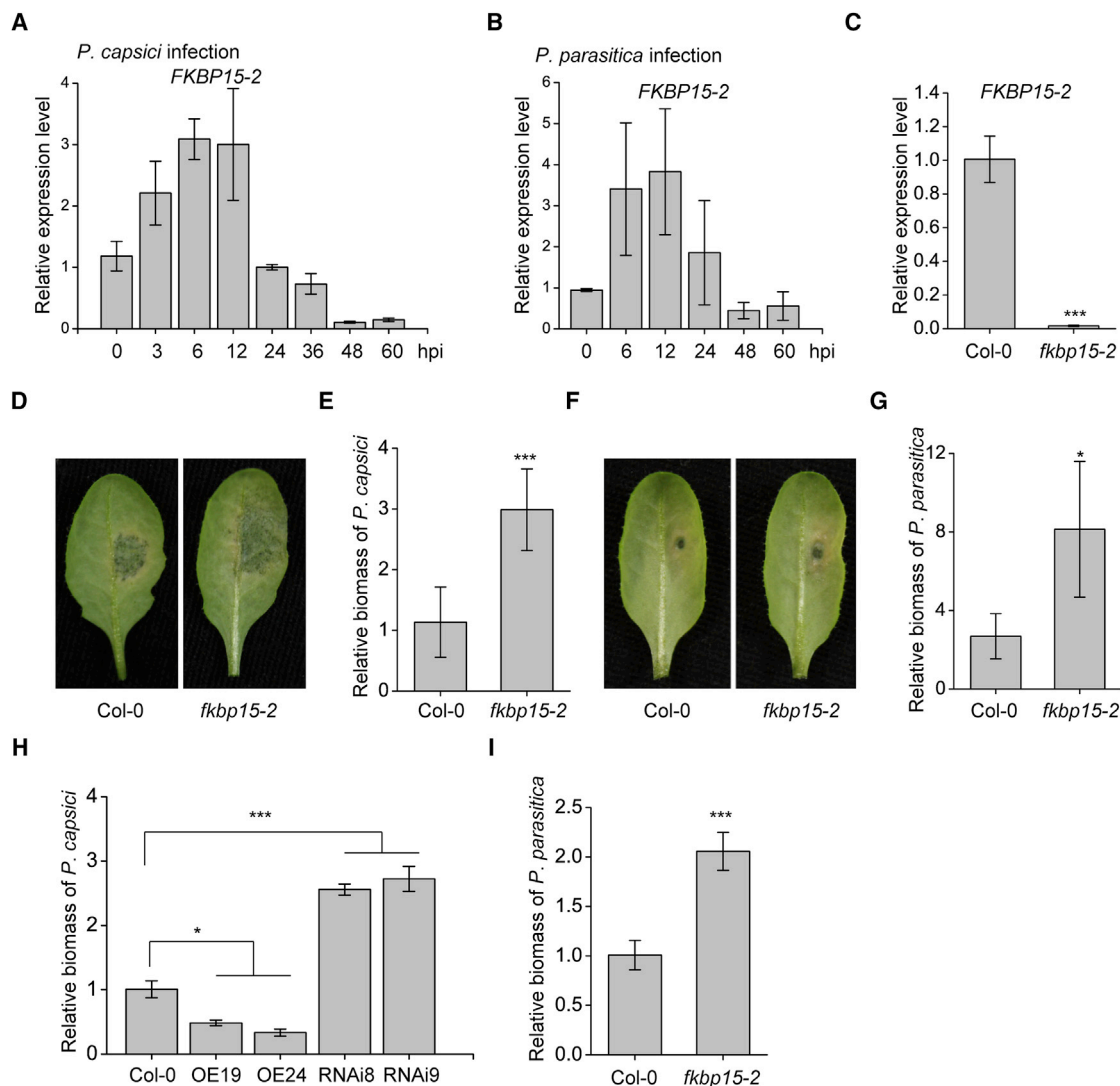


Figure 3. FKBP15-2 Positively Regulates *A. thaliana* Resistance to *Phytophthora* Pathogens.

(A and B) Expression of *FKBP15-2* at different stages during *P. capsici* or *P. parasitica* infection was determined by qRT-PCR. Four-week-old leaves from Col-0 were inoculated with *P. capsici* zoospores **(A)**. Total RNA was extracted from infected leaves at 0, 3, 6, 12, 24, 36, 48, and 60 hpi. Two-week-old roots of Col-0 were infected with zoospores from *P. parasitica* **(B)**. Total RNA was extracted from infected roots at 0, 6, 12, 24, 48, and 60 hpi. *A. thaliana UBC9* was used as an internal control. Error bars indicate SD of three biological replicates.

(C) The expression of *FKBP15-2* in the T-DNA insertion mutant *fkbp15-2* and the wild-type Col-0 as determined by qRT-PCR. Total RNA was extracted from leaves of 4-week-old plants. *UBC9* was used as an internal control. Error bars indicate SD of three biological replicates.

(D and F) Detached leaf inoculation assays showing that *fkbp15-2* is susceptible to *P. capsici* **(D)** and *P. parasitica* **(F)**. Images were taken at 60 hpi **(D)** and 72 hpi **(F)**.

(E and G) *P. capsici* or *P. parasitica* colonization of infected leaves at 60 or 72 hpi as determined by qRT-PCR. Primers specific for the *P. capsici* actin gene, the *P. parasitica UBC* gene (gene ID: PPTG_08 273), and the *A. thaliana UBC9* gene were used. Error bars indicate SD of three biological replicates, with at least eight leaves per replicate. Asterisks indicate significant differences (** $P < 0.01$, * $P < 0.05$).

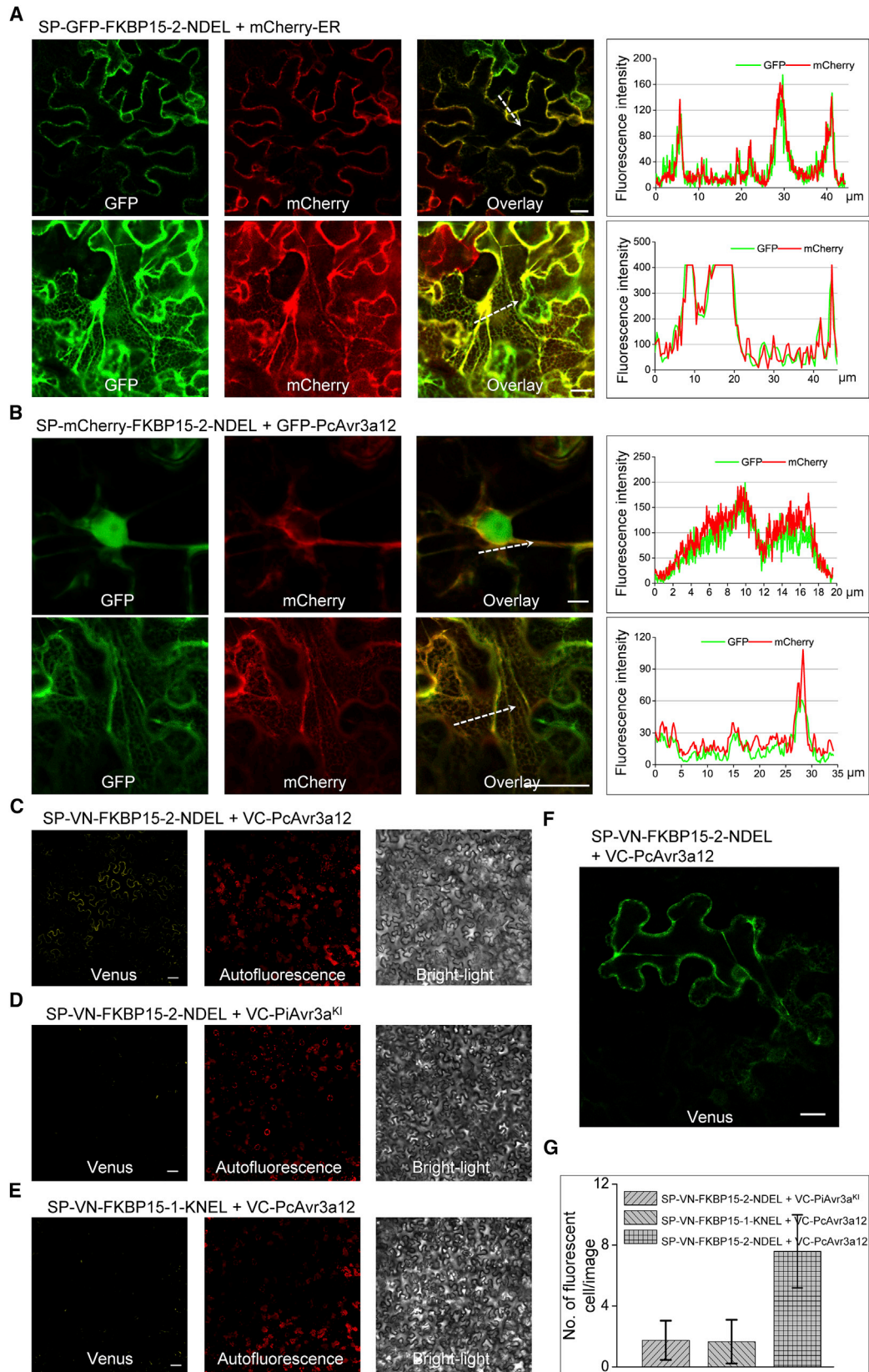
(H) *P. capsici* biomass in infected leaves of Col-0 and *FKBP15-2*-OE-19, *FKBP15-2*-OE-24, *FKBP15-2*-RNAi-8, and *FKBP15-2*-RNAi-9 lines at 60 hpi was determined by qRT-PCR. Error bars indicate SD of three biological replicates, with at least eight leaves per replicate. Asterisks indicate significant differences (** $P < 0.01$, * $P < 0.05$).

(I) *P. parasitica* colonization of infected *A. thaliana* roots. Total genomic DNA from *P. parasitica*-infected roots was isolated at 48 hpi. Error bars indicate SD of three biological replicates, with 24 seedling roots per replicate. Asterisks indicate significant differences (** $P < 0.01$).

1993; Yun et al., 2003), which were previously reported to be induced by *Phytophthora* infection (Attard et al., 2010; Wang et al., 2013), was reduced in *fkbp15-2* at least by 60% as compared with that in Col-0 at 6 hpi (Supplemental Figure 6). Taken together, these results show that *FKBP15-2* is required for plant resistance to *Phytophthora* infection in *A. thaliana*.

PcAvr3a12 Partially Associates with FKBP15-2 on the ER In Planta

To investigate the subcellular localization of *FKBP15-2* and its association with *PcAvr3a12*, we constructed plasmids to express mCherry or GFP fusions with each protein: p35S::GFP/mCherry-*PcAvr3a12* (*PcAvr3a12* SP was removed) and



(legend on next page)

p35S::SP-GFP/mCherry-FKBP15-2-NDEL. All these GFP/mCherry fusions were successfully expressed in *planta* as demonstrated by immunoblot analysis (Supplemental Figure 7A–7C). Consistent with a previous prediction (He et al., 2004), SP-directed GFP-FKBP15-2-NDEL completely overlapped with the mCherry-labeled ER marker in the perinuclear ER and the ER network (Figure 4A) when these proteins were co-expressed in *N. benthamiana* leaves. Moreover, GFP fluorescence in stable SP-GFP-FKBP15-2-NDEL-expressing *A. thaliana* leaves co-localized with ER-like networks and surrounded the nucleus (Supplemental Figure 8A), and no protein cleavage was observed (Supplemental Figure 8B). We observed that when GFP was tagged to the N terminus upstream of the SP, which abolished the proper function of SP, GFP-SP-FKBP15-2-NDEL SP was localized in the nucleus and cytoplasm (Supplemental Figure 9A and 9B), suggesting that the SP is required for ER localization of FKBP15-2.

When GFP-PcAvr3a12 (lacking the SP) was co-expressed with SP-directed mCherry-FKBP15-2-NDEL in *N. benthamiana* leaves, the two proteins partially overlapped at the peri-nuclear ER and the ER network, although GFP-PcAvr3a12 was also detectable in the cell nucleus and cytoplasm (Figure 4B). In addition, the plasma membrane- and nucleus-localized GFP-PiAvrblb2 (Bozkurt et al., 2011) did not overlap with the SP-directed mCherry-FKBP15-2-NDEL (Supplemental Figure 9C). Bimolecular fluorescence complementation (BiFC) assays, using N-terminal (VN) and C-terminal (VC) fragments of the Venus fluorescent protein, were used to confirm whether PcAvr3a12 associates with FKBP15-2 in live plant cells. FKBP15-1 and PiAvr3a^{KI} served as two independent controls in the BiFC assays. All fusion proteins were successfully expressed in *N. benthamiana* leaves without cleavage (Supplemental Figure 7D). Only the infiltrated leaves expressing SP-directed VN-FKBP15-2-NDEL and VC-PcAvr3a12 (lacking the SP) showed obvious fluorescence in the ER-like structures (Figure 4C and 4F) in contrast to all control constructs (Figure 4D and 4E). We observed significantly more fluorescing cells in leaves co-infiltrated with SP-VN-FKBP15-2-NDEL and VC-PcAvr3a12 as compared with the controls (Figure 4G). Taken together, these results suggest that PcAvr3a12 can at least partially associate with FKBP15-2 in the ER in live plant cells.

PcAvr3a12 and FKBP15-2 Co-localize around *Phytophthora* Haustoria during Infection

To further examine the subcellular localization of FKBP15-2 and PcAvr3a12 during *Phytophthora* infection, we inoculated *N. benthamiana* leaves expressing GFP or mCherry fusions with *Phytophthora* zoospores. Confocal microscopy showed that SP-directed mCherry-FKBP15-2-NDEL and mCherry-PcAvr3a12 proteins accumulated around the haustoria of GFP-labeled *P. parasitica* (Figure 5A and 5C; Supplemental Figure 10). Moreover, the ER was concentrated around haustoria during *Phytophthora* infection (Figure 5B). Consistent with this finding, GFP-PcAvr3a12 and SP-directed mCherry-FKBP15-2-NDEL were co-localized around haustoria-like structures after infection with *P. capsici* (Figure 5D). Using PiAvrblb2 as a marker of the extrahaustorial membrane during *Phytophthora* infection (Bozkurt et al., 2015), we further detected GFP-PcAvr3a12 co-localization with mCherry-PiAvrblb2 around haustoria-like structures (Figure 5E).

The PPlase Activity of FKBP15-2 Is Essential for Its Immune Function

It was previously reported that the FKBP15-2 ortholog in *Vicia faba* possesses PPlase activity (Luan et al., 1996). We therefore used a conventional protease-coupled PPlase assay to detect whether FKBP15-2 has PPlase activity. The 93rd residue (aspartic acid) in FKBP15-2 was predicted to be an essential site for PPlase activity based on previous analyses (Lucke and Weiwad, 2011; Supplemental Figure 11A). The maltose-binding protein (MBP) fusions, MBP-FKBP15-2, MBP-FKBP15-2^{D93A}, and MBP-GFP, were expressed in *Escherichia coli* and purified by binding to amylose resin columns, and protein expression was confirmed by both SDS-PAGE and immunoblot analysis (Supplemental Figure 11B). The purified proteins were incubated with *N*-succinyl-ala-ala-pro-pNa, which can be cleaved by α -chymotrypsin to yield colored 4-nitroaniline, only when the *N*-succinyl-ala-ala-pro-pNa prolyl bond is at trans-conformation. Compared with the spontaneous reaction, the accumulation of 4-Nitroaniline was faster with the addition of MBP-FKBP15-2 than with MBP-GFP (Figure 6A), indicating that FKBP15-2 possesses PPlase activity. Furthermore, the accumulation of 4-nitroaniline was slower with MBP-FKBP15-2^{D93A} than with MBP-FKBP15-2 (Figure 6A), consistent with loss of FKBP15-2^{D93A} PPlase activity.

Figure 4. *P. capsici* RXLR Effector PcAvr3a12 Associates with the Host Protein FKBP15-2 at the ER.

Proteins were expressed in *N. benthamiana* leaves through infiltration with an *A. tumefaciens* cell suspension with an OD₆₀₀ value of 0.3. Fluorescence in *N. benthamiana* epidermal cells was observed by confocal microscopy at 48 h post infiltration. Fluorescence plots show the relative fluorescence along the dotted line in the images.

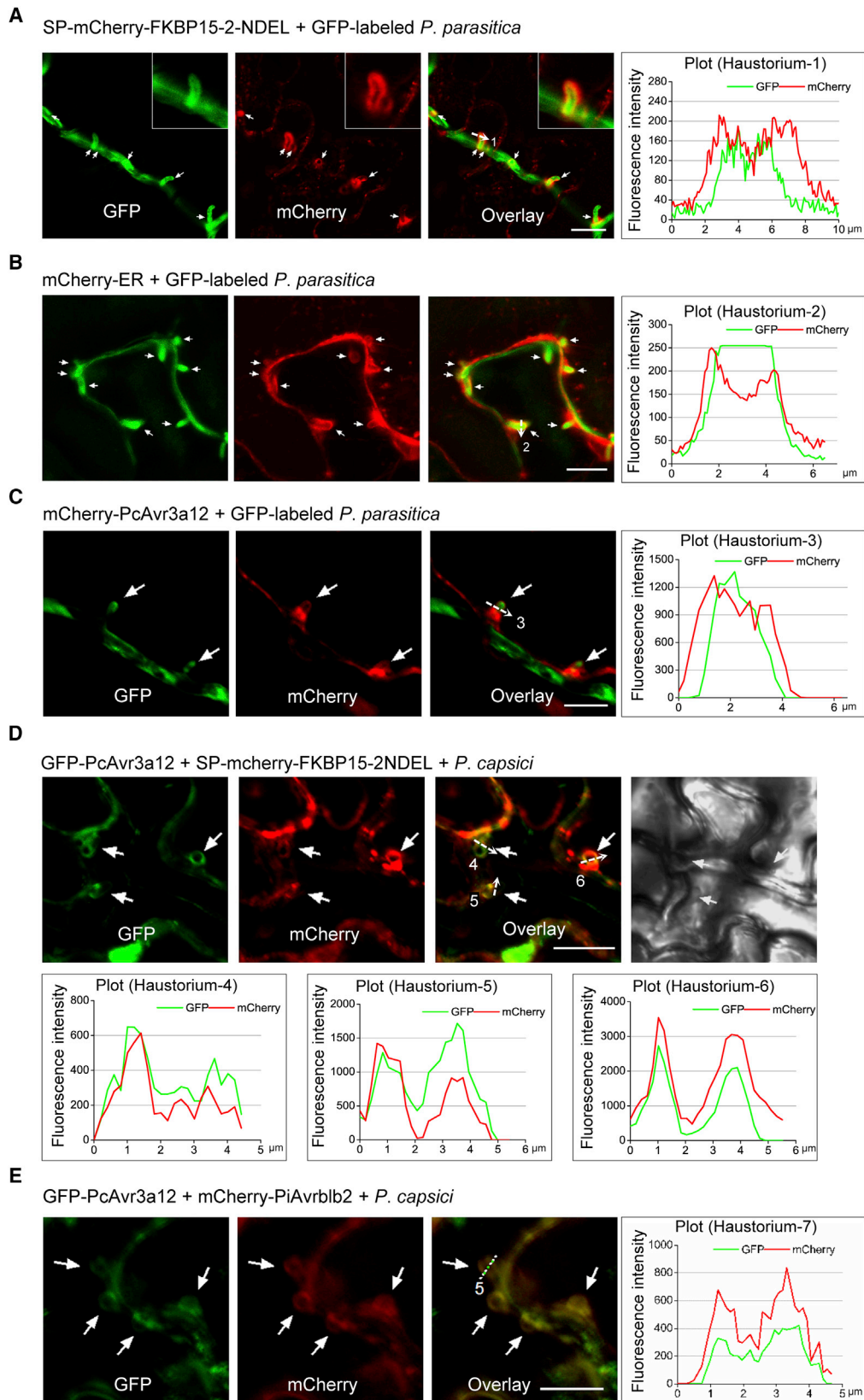
(A) SP-GFP-FKBP15-2-NDEL fluorescence overlaps with that of the mCherry-labeled ER marker at the peri-nuclear ER (upper panel) and the ER network (lower panel). Scale bar, 20 μ m.

(B) SP-mCherry-FKBP15-2-NDEL fluorescence partially overlaps with that of GFP-PcAvr3a12 at the peri-nuclear ER (upper panel) and the ER network (lower panel). Lower panel shows infiltration with an *A. tumefaciens* cell suspension with an OD₆₀₀ value of 0.1. Scale bar, 20 μ m.

(C–E) The interaction between PcAvr3a12 and FKBP15-2 in living cells was detected by BiFC. The C terminus of Venus (VC) was fused to the N terminus of PcAvr3a12 and PiAvr3a^{KI} (mature protein with the SP deleted), and the N terminus of Venus (VN) was fused between the secretory SP and FKBP15-2-NDEL or FKBP15-1-KNEL. Co-expression of SP-VN-FKBP15-2-NDEL and VC-PcAvr3a12 resulted in specific fluorescence as detected by confocal microscopy (C), in contrast to two control combinations (D and E). Three independent experiments showed similar results. Scale bars, 40 μ m.

(F) Enlarged image shows a representative fluorescent cell expressing SP-VN-FKBP15-2-NDEL and VC-PcAvr3a12. Scale bar, 20 μ m.

(G) Quantitative statistical analysis of the average number of fluorescent cells per observable field using 20 \times magnification and identical settings for each of the replicates. Significantly more fluorescent cells were observed in leaves co-expressing SP-VN-FKBP15-2-NDEL and VC-PcAvr3a12 as compared with those expressing control combinations ($P < 0.001$, t -test, $n = 12$ fields of view for each pair).



(legend on next page)

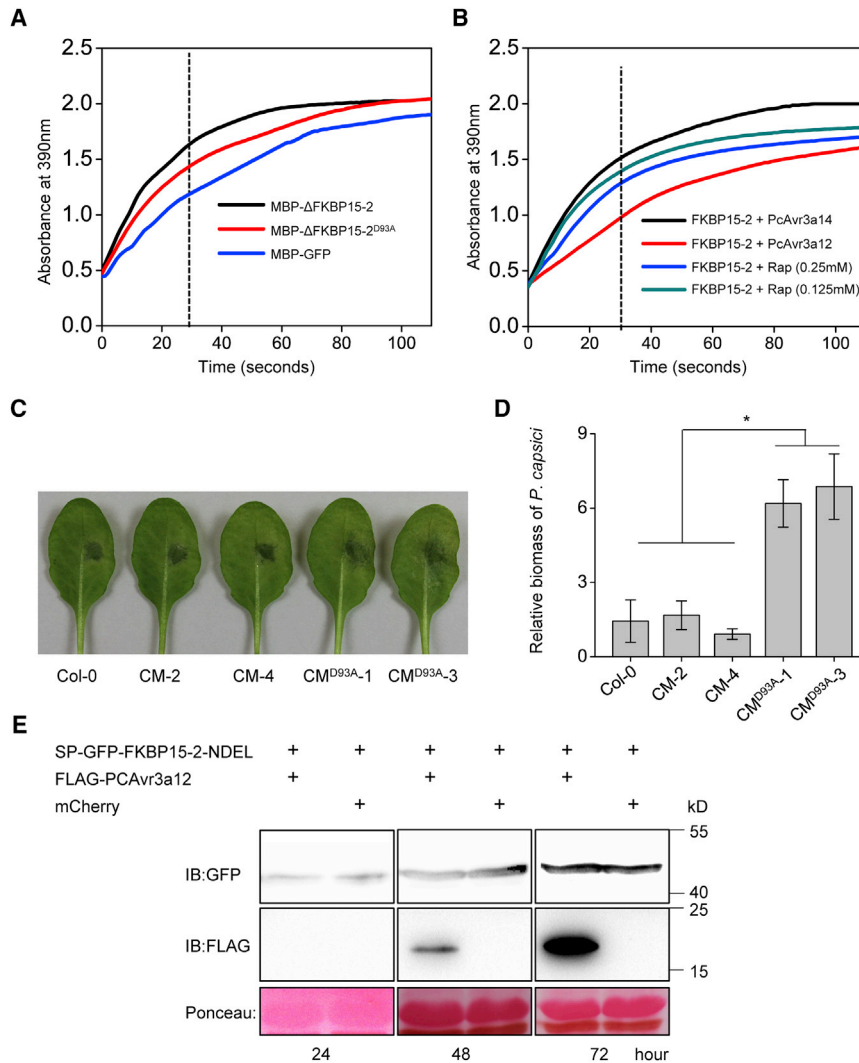


Figure 5. *P. capsici* Effector PcAvr3a12 and Host Protein FKBP15-2 Accumulate Around Haustoria during *Phytophthora* Infection. Each construct was expressed in *N. benthamiana* leaves through infiltration with an *A. tumefaciens* cell suspension (OD₆₀₀ of 0.2–0.3). Infiltrated leaves were inoculated with *P. capsici* or GFP-expressing *P. parasitica* zoospores at 24 h post infiltration. Fluorescence was observed by confocal microscopy at 60 h post infiltration. GFP and mCherry signals are indicated in green and red, respectively. White arrows indicate *Phytophthora* haustoria. The fluorescence plots show the relative fluorescence along the dotted line in the images. Three independent biological replicates showed similar results. Scale bars, 10 μm. (A) Fluorescence of SP-mCherry-FKBP15-2-NDEL indicates its accumulation around haustoria during infection with GFP-labeled *P. parasitica*. (B) Fluorescence of an ER marker indicates haustoria surrounded by the ER during infection with GFP-labeled *P. parasitica*. (C) Fluorescence of mCherry-PcAvr3a12 indicates its accumulation around haustoria during infection with GFP-labeled *P. parasitica*. (D) GFP-PcAvr3a12 and SP-mCherry-FKBP15-2-NDEL co-localize around haustoria following inoculation with *P. capsici*. (E) Localization of GFP-PcAvr3a12 and mCherry-PiAvrblb2 around haustoria following infection with *P. capsici*.

To confirm whether the PPIase activity of FKBP15-2 is required for its contribution to immunity, we complemented *fbp15-2* mutant *A. thaliana* line by transforming them with *pFKBP15-2::FKBP15-2* or *pFKBP15-2::FKBP15-2^{D93A}*. Two independent

pFKBP15-2::FKBP15-2 complementation lines (CM) and two independent *pFKBP15-2::FKBP15-2^{D93A}* mutant complementation lines (CM^{D93A}) were confirmed by quantitative RT-PCR (qRT-PCR) (Supplemental Figure 5F) and were chosen for infection

Figure 6. PPIase Activity of FKBP15-2 Is Required for Its Immune Function During *Phytophthora* Infection.

(A) PPIase activity of FKBP15-2 and FKBP15-2^{D93A}. The recombinant proteins MBP-GFP, MBP-ΔFKBP15-2, and MBP-ΔFKBP15-2^{D93A} were expressed and purified from *E. coli*. “Δ” indicates specific protein constructs in which the SP and the potential ER retention signal were deleted. PPIase activities were analyzed by chymotrypsin-coupled assay at 8°C using succinyl-Ala-Leu-Pro-Phe-*p*-nitroanilide as the substrate. Faster appearance of the absorbance in 390 nm is indicative of higher PPIase activity. Enzyme activity can be assessed by analyzing the peak of the curve 24s (dotted line indicated) after the adding of α-chymotrypsin. The final concentration of each purified protein in the mix was 10 iM. MBP-GFP was used as a control. Three independent replicates showed similar results. (B) PPIase activity assay for MBP-ΔFKBP15-2 in the presence of PcAvr3a14, rapamycin, or PcAvr3a12. The recombinant proteins MBP-FKBP15-2, MBP-PcAvr3a12, and MBP-PcAvr3a14 were expressed and purified from *E. coli*. MBP-PcAvr3a14 and rapamycin, which is a chemical suppressor of PPIases, were used as controls. The final concentration of each purified protein in the mix, including MBP-FKBP15-2, MBP-PcAvr3a12, and MBP-PcAvr3a14, was 10 iM. PPIase activity was analyzed with a chymotrypsin-coupled assay at 8°C using succinyl-Ala-Leu-Pro-Phe-*p*-nitroanilide as the substrate. Faster appearance of an absorbance peak at 390 nm is indicative of higher PPIase activity. Three independent experiments showed similar results. (C) Detached leaves of *FKBP15-2* mutant complementation lines (CM^{D93A}) showing enhanced susceptibility to infection by *P. capsici* zoospores. Representative images were taken at 60 hpi.

(D) *P. capsici* biomass in infected leaves of Col-0, *FKBP15-2* complementation lines (CM), and *FKBP15-2* mutant complementation lines (CM^{D93A}) at 60 hpi, as determined by qRT-PCR. Error bars indicate SD from three biological replicates. Asterisks indicate significant differences (**P* < 0.05).

(E) Protein stability of FKBP15-2, co-expressed with PcAvr3a12 or mCherry, was analyzed by immunoblotting (IB). The SP-GFP-FKBP15-2-NDEL protein was co-expressed with FLAG-PcAvr3a12 or mCherry in *N. benthamiana* leaves through agroinfiltration. Total proteins were extracted from infiltrated leaves at 1, 2, and 3 days post agroinfiltration. SP-GFP-FKBP15-2-NDEL and FLAG-PcAvr3a12 were detected by immunoblotting using anti-GFP- and FLAG-antibodies, respectively. Ponceau staining of the membrane was used to show equal loading.

Figure 6. PPIase Activity of FKBP15-2 Is Required for Its Immune Function During *Phytophthora* Infection.

(A) PPIase activity of FKBP15-2 and FKBP15-2^{D93A}. The recombinant proteins MBP-GFP, MBP-ΔFKBP15-2, and MBP-ΔFKBP15-2^{D93A} were expressed and purified from *E. coli*. “Δ” indicates specific protein constructs in which the SP and the potential ER retention signal were deleted. PPIase activities were analyzed by chymotrypsin-coupled assay at 8°C using succinyl-Ala-Leu-Pro-Phe-*p*-nitroanilide as the substrate. Faster appearance of the absorbance in 390 nm is indicative of higher PPIase activity. Enzyme activity can be assessed by analyzing the peak of the curve 24s (dotted line indicated) after the adding of α-chymotrypsin. The final concentration of each purified protein in the mix was 10 iM. MBP-GFP was used as a control. Three independent replicates showed similar results. (B) PPIase activity assay for MBP-ΔFKBP15-2 in the presence of PcAvr3a14, rapamycin, or PcAvr3a12. The recombinant proteins MBP-FKBP15-2, MBP-PcAvr3a12, and MBP-PcAvr3a14 were expressed and purified from *E. coli*. MBP-PcAvr3a14 and rapamycin, which is a chemical suppressor of PPIases, were used as controls. The final concentration of each purified protein in the mix, including MBP-FKBP15-2, MBP-PcAvr3a12, and MBP-PcAvr3a14, was 10 iM. PPIase activity was analyzed with a chymotrypsin-coupled assay at 8°C using succinyl-Ala-Leu-Pro-Phe-*p*-nitroanilide as the substrate. Faster appearance of an absorbance peak at 390 nm is indicative of higher PPIase activity. Three independent experiments showed similar results. (C) Detached leaves of *FKBP15-2* mutant complementation lines (CM^{D93A}) showing enhanced susceptibility to infection by *P. capsici* zoospores. Representative images were taken at 60 hpi.

(D) *P. capsici* biomass in infected leaves of Col-0, *FKBP15-2* complementation lines (CM), and *FKBP15-2* mutant complementation lines (CM^{D93A}) at 60 hpi, as determined by qRT-PCR. Error bars indicate SD from three biological replicates. Asterisks indicate significant differences (**P* < 0.05). (E) Protein stability of FKBP15-2, co-expressed with PcAvr3a12 or mCherry, was analyzed by immunoblotting (IB). The SP-GFP-FKBP15-2-NDEL protein was co-expressed with FLAG-PcAvr3a12 or mCherry in *N. benthamiana* leaves through agroinfiltration. Total proteins were extracted from infiltrated leaves at 1, 2, and 3 days post agroinfiltration. SP-GFP-FKBP15-2-NDEL and FLAG-PcAvr3a12 were detected by immunoblotting using anti-GFP- and FLAG-antibodies, respectively. Ponceau staining of the membrane was used to show equal loading.

Molecular Plant

assays with *P. capsici* zoospores. The water-soaked lesions on leaves of CM lines and Col-0 were smaller than those on the leaves of CM^{D93A} lines (Figure 6C), which had less pathogen colonization at 60 hpi (Figure 6D), while the water-soaked lesions on leaves of CM lines and Col-0 were similar (Figure 6C) with no significant difference in pathogen colonization (Figure 6D). These results indicate that the PPlase activity of FKBP15-2 is required for its contribution to immunity against *Phytophthora*.

PcAvr3a12 Directly Suppresses the PPlase Activity of FKBP15-2

Based on our finding that the PPlase activity of FKBP15-2 is essential for its contribution to immunity, we investigated whether this activity is affected by PcAvr3a12 in a protease-coupled *in vitro* assay. Expression of all purified recombinant proteins used in these PPlase activity assays was confirmed by SDS-PAGE and immunoblots (Supplemental Figure 11C). The PPlase activity of MBP-FKBP15-2 incubated with MBP-PcAvr3a12, MBP-PcAvr3a14, and rapamycin (a chemical inhibitor of PPlase), respectively, was assayed as previously described (Harding et al., 1989). Here, MBP-PcAvr3a14 and rapamycin were used as controls. In the presence of PcAvr3a12 or rapamycin, the PPlase activity of MBP-FKBP15-2 was lower than that in the presence of PcAvr3a14 (Figure 6B), suggesting that the PPlase activity of FKBP15-2 was attenuated by binding to PcAvr3a12. We also examined whether PcAvr3a12 affects the *in vivo* stability of FKBP15-2. The FKBP15-2-GFP fusion was co-transformed with FLAG-PcAvr3a or free mCherry into *N. benthamiana* leaves by agroinfiltration. We found that the accumulation of SP-directed GFP-FKBP15-2-NDEL was not significantly different between the leaves co-expressing FLAG-PcAvr3a12 and mCherry (Figure 6E).

FKBP15-2 Is Involved in General UPR Induction and ER Stress-Mediated Plant Immunity

The protein folding capacity of the ER has been demonstrated to be crucial for rapid and effective basal immune responses (Körner et al., 2015). Our findings that FKBP15-2 is localized in the ER and has PPlase activity prompted us to question whether FKBP15-2 mediates immunity against *Phytophthora* spp by regulating ER stress. To test this, we treated 5-day-old seedlings of Col-0 and the *fkbp15-2* mutant with the ER stress inducer/*N*-glycosylation inhibitor tunicamycin (TM) or dimethyl sulfoxide (DMSO) as a control. At 7 days post treatment, the fresh weight of the seedlings was measured. There was around a 50% reduction in the fresh weight of the TM-treated Col-0 seedlings compared with that of the DMSO-treated seedlings. In contrast, in the *fkbp15-2* mutants, TM treatment resulted in only about a 17% biomass reduction compared with control seedlings (Figure 7C), suggesting that FKBP15-2 might contribute to the sensing of TM-induced ER stress.

To further examine whether FKBP15-2 contributes to ER stress sensing and subsequent UPR regulation, we spray-treated 12-day-old Col-0 and *fkbp15-2* seedlings with TM, and monitored via real-time qRT-PCR the transcript levels of the ER stress sensor genes *bZIP60* and *bZIP28* and the UPR marker gene *BiP3*. We found that the levels of *bZIP60*, spliced *bZIP60* (ER stress-activated form of *bZIP60*), and *BiP3* were significantly elevated in Col-0 treated with TM. However, the increase in *bZIP60*,

PcAvr3a12 Targets and Inhibits a Plant PPlase

spliced *bZIP60*, and *BiP3* transcript levels was significantly attenuated in the *fkbp15-2* mutants at 6 h post TM treatment (Figure 7A). Although *bZIP28* expression was not clearly elevated by TM treatment, its transcript level was reduced in the *fkbp15-2* mutants as compared with Col-0 (Figure 7A). These results indicate that FKBP15-2 contributes to general ER stress sensing and UPR regulation, although there was no obvious elevation of FKBP15-2 transcript levels in the TM-treated Col-0 (Supplemental Figure 12B).

To investigate whether the contribution of FKBP15-2 to immunity is related to its contribution to ER stress and UPR regulation, we examined the transcript levels of the ER stress sensor genes *bZIP60*, *bZIP28*, and *BiP3* during early biotrophic colonization by *P. capsici*. For these qRT-PCR analyses, leaves of 4-week-old Col-0 and *fkbp15-2* mutants were inoculated with *P. capsici* zoospores and harvested at 0, 3, 6, and 12 hpi. We found that the levels of *bZIP60* and *BiP3* transcripts in Col-0 were elevated at early stages of infection by *P. capsici*, while only a slight increase in *bZIP28* expression, if any, was observed. In contrast, the transcription of *bZIP60*, *bZIP28*, and *BiP3* in the *fkbp15-2* mutants was significantly attenuated during early infection by *P. capsici* (Figure 7B). In accordance with this, several immunity-related genes were obviously induced upon infection by *P. capsici* in the Col-0 plants, including *avPE* (ER stress-mediated cell death gene), *WRKY33* (UPR-mediated SAR priming gene), *EFR* (ER-QC-dependent pattern-recognition receptor), and *CYP81F2* (a *P. capsici* resistance gene encoding an ER-localized indole glucosinolate biosynthesis enzyme gene; Wang et al., 2013) (Figure 7B). However, in the *fkbp15-2* mutant the increase in transcription of *WRKY33*, *EFR*, and *CYP81F2* was significantly reduced during early infection compared with that in Col-0, especially at 6 and 12 hpi (Figure 7B). Similarly, when 12-day-old seedlings were inoculated with *P. parasitica*, the expression levels of ER stress sensors (*bZIP60* and *bZIP28*) and ER stress-mediated immunity genes (*avPE*, *WRKY33* and *EFR*) were lower during early infection in *fkbp15-2* mutants compared with Col-0 (Supplemental Figure 12A). Taken together, these results imply that FKBP15-2 contributes to ER stress-mediated plant immunity.

DISCUSSION

Plant pathogens secrete effectors to interfere with plant immune responses and promote colonization (Jones and Dangl, 2006). PiAvr3a is a well-known RXLR effector from *P. infestans* that plays an essential role in pathogenesis (Bos et al., 2010; Gilroy et al., 2011; Chaparro-Garcia et al., 2015). Avr3a family effectors are among the few RXLR effectors that are relatively well conserved across diverse *Phytophthora* species, and this family is highly expanded in *P. capsici* (Bos, 2007), suggesting that these effectors are important in pathogenesis and that they may have evolved specialized roles in *P. capsici* (Vega-Arreguin et al., 2014). We found that PcAvr3a12 is highly upregulated during early infection, and expression *in planta* renders the host plant *A. thaliana* more susceptible to *P. capsici* (Figure 1), supporting its role as a virulence effector, consistent with the virulence role of the Avr3a family effectors PiAvr3a (Bos et al., 2010) and PsAvr1b (Dou et al., 2008). In contrast to PiAvr3a and PsAvr1b, respectively, PcAvr3a12 cannot be recognized by R3a or suppress INF1-triggered cell death (Supplemental Figure 1), suggesting it has evolved a more specialized role in

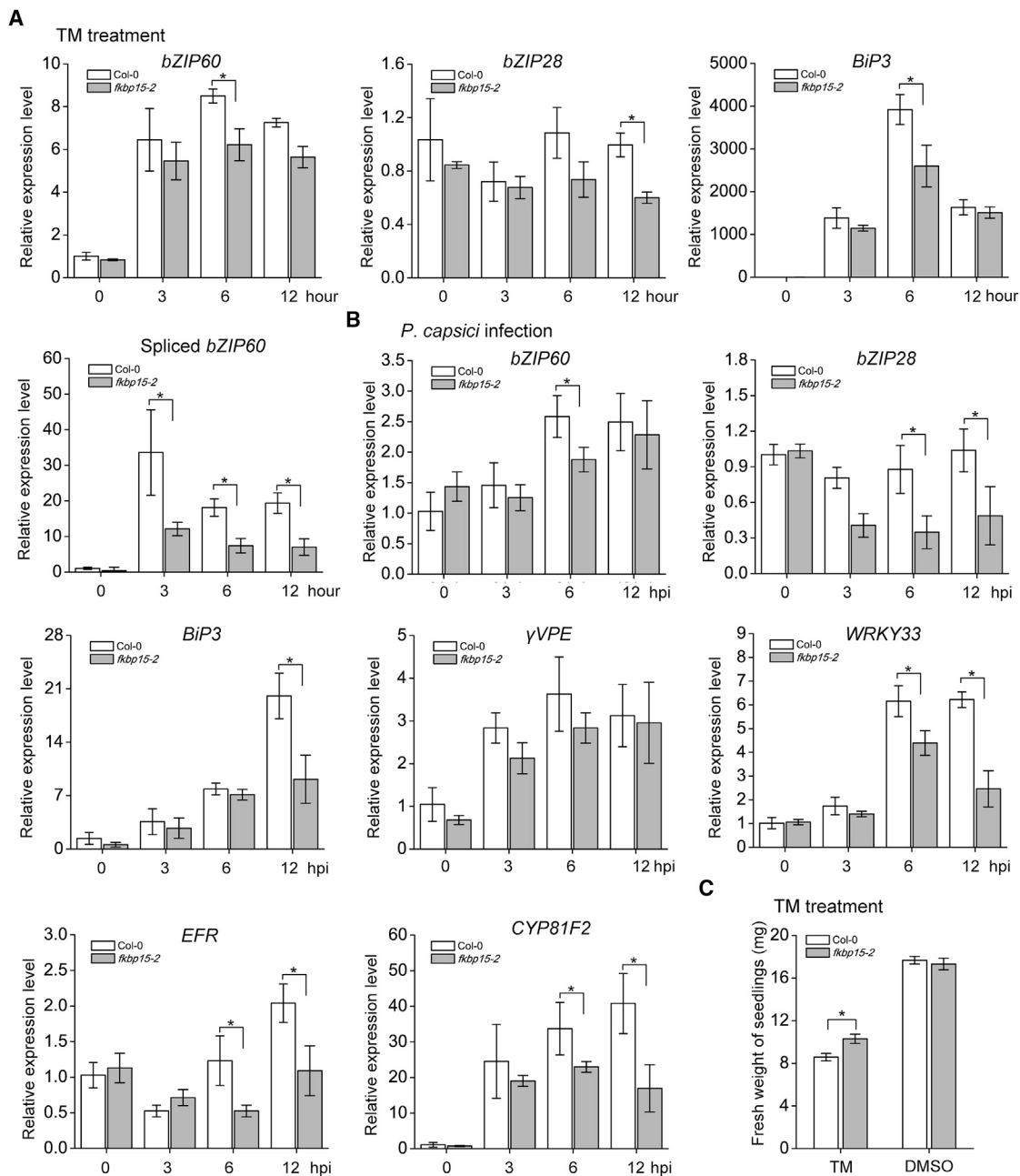


Figure 7. FKBP15-2 Is Involved in UPR and ER Stress-Mediated Plant Immunity During *Phytophthora* Infection.

(A) The dynamic expression of *bZIP60*, *bZIP28*, *BiP3*, and spliced *bZIP60* was evaluated by qRT-PCR. Ten-day-old seedlings of wild-type Col-0 and *fkbp15-2* mutants were sprayed with TM (5 μ g/ml). Total RNA was extracted from seedlings at 0, 3, 6, and 12 h post treatment. *UBC9* was used as the plant reference gene. Error bars indicate SD from three biological replicates. Asterisks indicate significant differences ($*P < 0.05$).

(B) Expression levels of *bZIP60*, *bZIP28*, γ VPE, *WRKY33*, *CYP81F2*, and *EFR* were determined by qRT-PCR. Detached leaves of 4-week-old plants of wild-type Col-0 and *fkbp15-2* mutants were inoculated with *P. capsici* zoospores. Total RNA was extracted from leaves at 0, 3, 6, and 12 hpi. *UBC9* was used as the plant reference gene. Error bars indicate SD of three biological replicates. Asterisks indicate significant differences ($*P < 0.05$).

(C) Fresh weight of *fkbp15-2* and Col-0 under TM-triggered ER stress. Four-day-old wild-type Col-0 and *fkbp15-2* mutant seedlings were grown in liquid medium with TM (50 μ g/ml), using DMSO as a negative control. Seedling fresh weight was determined at 7 days post treatment. For each sample, at least 12 seedlings were used. Three independent experiments showed similar results. Error bars indicate SD from 12 seedlings. Asterisks indicate significant differences ($*P < 0.01$).

P. capsici. Accordingly, PcAvr3a12 was found to have a distinct host target, AtFKBP15-2, that we identified through Y2H screening and further confirmed through Y2H, CoIP, and BiFC assays (Figures 2 and 4C–4G).

In plants there are three PPIase families: cyclophilins (CYPs), FK506- and rapamycin-binding proteins (FKPBs), and parvulins (He et al., 2004). Two plant CYPs, ROC1 (Coaker et al., 2005) and GmCYP1 (Kong et al., 2015), were found to be required for

activation of specific effectors by mediating allosteric transition of effector peptidyl–prolyl bonds. In the case of PcAvr3a12, however, there is no proline in the mature protein, consistent with a different mechanism of interaction between FKBP15-2 and PcAvr3a12.

FKBP family members are involved in diverse aspects of cellular physiology including hormone signaling, protein trafficking, transcription, plant growth, and stress response (Harrar et al., 2001; Romano et al., 2005). However, the specific roles of many FKBP family members in plants remain unclear (Vasudevan et al., 2015). *AtFKBP65*, a homolog of *AtFKBP15-2*, was recently reported to be responsive to *Pseudomonas syringae* infection and to be required for callose accumulation (Pogorelko et al., 2014). We found that *FKBP15-2* is responsive to *Phytophthora* infection (Figure 3A and 3B) and positively contributes to plant resistance (Figure 3C–3I). We have also detected FKBP15-2 peptidyl–prolyl *cis-trans* isomerase activity in protease-coupled assays (Figure 6A), as reported for its ortholog in *V. faba* (Luan et al., 1996). In accordance with previous work (Lucke and Weiwad, 2011), mutating an essential residue (FKBP15-2^{D93A}) weakened its PPIase activity (Figure 6A). Further pathogenicity assays on *FKBP15-2*^{D93A} and *FKBP15-2* complementation lines showed that the PPIase activity of FKBP15-2 is important for its immunity-associated function against *Phytophthora* infection (Figure 6C and 6D). Based on this, together with our finding that PcAvr3a12 directly suppresses the PPIase activity of FKBP15-2 *in vitro* (Figure 6B), we conclude that PcAvr3a12 attenuates plant immunity by suppressing the PPIase activity of FKBP15-2.

Trans-cis isomerization activity mediated by PPIases is crucial for protein folding, since the majority of proteins have prolyl residues (Braakman and Hebert, 2013). It is well documented that proline isomerization is a slow process and rate-limiting for protein folding (Brandts et al., 1977; Lang et al., 1987). In addition, ER-localized molecular chaperones and foldases generally form complexes to modulate protein modification and folding, which is an important part of the UPR (Jansen et al., 2012). The ER-localized BiP chaperones regulate UPR signaling after dissociation from the ER stress sensor IRE1 (Bertolotti et al., 2000). Both *VfFKBP15* from *V. faba* and *ScFKBP2* from *Saccharomyces cerevisiae* are orthologs of *AtFKBP15-2* and *AtFKBP15-1*. The *VfFKBP15* gene was highly upregulated under heat-shock stress (Luan et al., 1996), and *ScFKBP2* was highly upregulated after treatment with the ER stress inducer tunicamycin (TM) (Partaledis and Berlin, 1993), implying that these genes have a key role in protein folding. In contrast, there was no obvious induction of *AtFKBP15-2* in Col-0 by TM treatment (Supplemental Figure 12B), implying a different role of *AtFKBP15-2* in *A. thaliana* or, alternatively, post-transcriptional regulation of *AtFKBP15-2*. In our study, the *fkbp15-2* mutants exhibited insensitivity to TM treatment (Figure 7C). Furthermore, the TM-triggered induction of ER stress sensor genes (*bZIP60*, spliced *bZIP60*, and *bZIP28*) and a UPR marker gene (*BiP3*) was significantly reduced in the *fkbp15-2* mutants compared with Col-0 (Figure 7A). These results suggest that *FKBP15-2* is (directly or indirectly) involved in the transcription of the ER stress sensors *bZIP60* and *bZIP28* and subsequent regulation of UPR pathways. FKBP family members not only help in protein folding but also modulate signal transduction pathways by changing the activity of interacting proteins (Harrar et al., 2001). Thus, further

identification of FKBP15-2-interacting proteins will facilitate the elucidation of the mechanisms by which FKBP15-2 affects transcription of ER stress sensors and regulation of the UPR pathways.

There is clear evidence that ER stress response contributes to plant immunity in several ways, for example, through the processing pattern-recognition receptors, the regulation of antimicrobial protein secretion, and priming of SAR- and ER stress-mediated cell death (Wang et al., 2005; Li et al., 2009; Moreno et al., 2012; Qiang et al., 2012; Kørner et al., 2015). It was recently shown that GmBiPs are targeted by the *P. sojae* RXLR effector PsAvh262, resulting in the attenuation of ER stress-mediated cell death (Jing et al., 2016), which suggests that one way that microbes achieve compatibility is through manipulation of plant ER stress by effectors. In addition to altered expression of ER stress sensing and UPR marker genes (Figure 7B), mutants lacking the PcAvr3a12 target FKBP15-2 displayed attenuated induction of two known ER stress-mediated plant immunity marker genes, *EFR* and *WRKY33*, during the early stages of *Phytophthora* infection (Figure 7B and Supplemental Figure 12A). Furthermore, transcription of the ER stress-mediated cell death marker gene *αVPE* was attenuated in *fkbp15-2* mutants during the early stages of infection by *P. parasitica* (Supplemental Figure 12A), as was the expression of secreted immunity-related protein genes (*PR1* and *PDF1.2*) (Supplemental Figure 6) and the ER-localized *P. capsici* resistance gene *CYP81F2* (Wang et al., 2013) (Figure 7B) in *fkbp15-2* mutants in the early stages of *P. capsici* infection. These results suggest that *FKBP15-2* positively contributes to plant resistance, most likely by participating in ER stress response pathways. Future studies of *P. capsici* strains with silencing or knockout of *PcAvr3a12* may further confirm whether this effector directly disturbs the host UPR.

Since the SP of FKBP15-2 is essential for its ER localization (Figure 4A and Supplemental Figure 9), it is likely that the translation of FKBP15-2 is completed at the ER and thus most FKBP15-2 reaches the ER by the co-translational pathway. This may explain why PcAvr3a12 is not significantly enriched in the ER during co-expression with FKBP15-2 (Figure 4B). Our subcellular localization (Figure 4B) and BiFC (Figure 4C–4G) assays indicate that even when lacking its SP, some PcAvr3a12 protein overlaps with FKBP15-2 in the ER in healthy plant cells. How PcAvr3a12 enters the ER structures when it is expressed at high levels in plant cells remains unclear. It is possible that a fraction of FKBP15-2 is post-translationally targeted to the ER, and that this fraction is sufficient to bind to PcAvr3a12 and carry it into the ER. During natural infection, effectors are thought to enter plant cells via some form of endocytosis, which would target them to the lumen of the endomembrane system, where they could undergo retrograde trafficking to the ER. Currently, it is difficult to directly observe the translocation route and subcellular localization of *Phytophthora* effectors during infection (Wang et al., 2017). However, our localization assays of FKBP15-2 and PcAvr3a12 during infection showed that both proteins accumulated and co-localized around haustoria, further supporting their interaction (Figure 5 and Supplemental Figure 10). Taken together, we propose that during early infection *P. capsici* secretes the RXLR effector PcAvr3a12, which targets the ER-localized PPIase FKBP15-2 around haustoria, to suppress plant

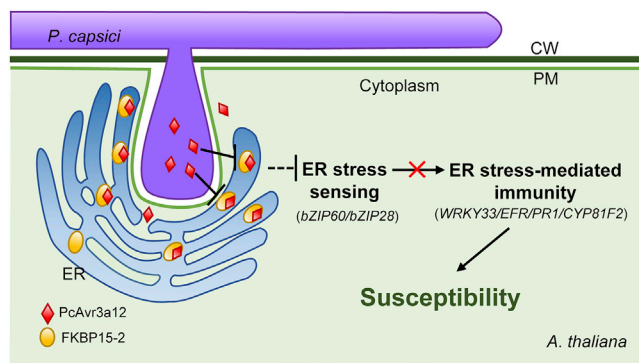


Figure 8. A Schematic Model of the Role of FKBP15-2 and PcAvr3a12 in Plant Immunity to *Phytophthora*.

P. capsici develops haustoria that secrete and deliver effectors, including PcAvr3a12, into host cells to manipulate host cell function. Plant ER-localized PPIase, FKBP15-2, accumulates and surrounds haustoria. FKBP15-2 is directly targeted and inhibited by PcAvr3a12 around haustoria. *Phytophthora* infection activates an ER stress response and ER stress-mediated immunity in plants. The T-DNA insertion mutant *fkbp15-2* shows significantly attenuated expression of *bZIP60* and *bZIP28* and multiple ER-processed immune genes (e.g., *aVPE*, *EFR*, *WRKY33*, and *PR1*). Based on these results, we propose that the *P. capsici*-secreted RXLR effector PcAvr3a12 circumvents plant immunity by targeting and suppressing a novel ER-localized immune protein, FKBP15-2, that positively regulates plant resistance by participating in ER stress-mediated plant immunity. CW, cell wall; PM, plasma membrane; H, haustoria; ER, endoplasmic reticulum.

immunity (Figure 8). Targeting of FKBP15-2 seems to be especially relevant for *P. capsici* infection due to its participation in maintaining ER homeostasis.

METHODS

Plasmid Constructs

For the creation of Y2H constructs, the coding regions of *AtFKBP15-2*, *AtFKBP15-1*, *PcAvr3a12*, *PcAvr3a14*, and *PcFKBP35* without the secretion SP and the ER retention peptide were cloned from Col-0 or LT263 cDNA and inserted into the *EcoRI* and *BamHI* sites of pGADT7 and pGBKT7. For the creation of BiFC constructs, the fusion fragments SP-VN-FKBP15-2-NDEL and SP-VN-FKBP15-1-KDEL were obtained through overlapping PCR and inserted into the *SpeI* and *SacI* sites of pDEST-GWVYNE (Gehl et al., 2009). The coding sequences of *PcAvr3a12* and *PiAvr3a^{KI}* without the SP were inserted into the *SpeI* and *XhoI* sites of pDEST-VYCE^{GW} (Gehl et al., 2009). For preparation of overexpression constructs, the full-length *FKBP15-2* sequence was cloned from Col-0 cDNA and inserted into the *EcoRI* and *BamHI* sites of pKannibal (Wesley et al., 2001), then inserted into the binary vector pART27 (Gleave, 1992) at the *NotI* site. To create eGFP/mCherry/7*myc-fusion plasmids, we first cloned the eGFP/mCherry/7*myc fragment into pKannibal with *XhoI* and *EcoRI* sites and use the *NotI* sites to release the fragment with the promoter and terminator and then inserted it into pART27 vector. The mature PcAvr3a12 and full-length FKBP15-2 coding sequences were inserted into previously modified pART27 at the *EcoRI* and *XbaI* sites to create *GFP/mCherry/7*myc-PcAvr3a12* and *GFP-SP-FKBP15-2-NDEL*. For other plant expression constructs, including *SP-GFP/mCherry-FKBP15-2-NDEL*, *FLAG-PiAvr3a^{KI}*, and *FLAG-PcAvr3a12*, fusion fragments were obtained from restriction enzyme digestion or overlapping PCR and cloned into the *XhoI* and *XbaI* sites of the previously described plant expression vector, replacing the existing sequence. To generate the RNA silencing vector, we chose a specific 250-bp fragment – with no predicted off-target effects and inserted

it into the pKannibal vector between the *XhoI*–*EcoRI* sites in the sense orientation and between the *Clal*–*XbaI* sites in the antisense orientation to create a hairpin. Finally, this hairpin was transferred into pART27 at the *NotI* site. To construct the *pFKBP15-2::GUS* reporter vector, we amplified a 1097-bp promoter fragment of *FKBP15-2* from Col-0 genomic DNA and inserted it into the *KpnI* and *ASCI* sites of the pMDC162 binary vector (Curtis and Grossniklaus, 2003). We constructed other *pFKBP15-2* promoter-derived vectors, including *pFKBP15-2::FKBP15-2* and *pFKBP15-2::FKBP15-2^{D93A}*, by replacing the *GUS* sequence using the *ASCI* and *SacI* sites. The plant expression vector containing the ER marker was obtained from ABRC (stock number CD3-959) (Nelson et al., 2007). To create prokaryotic expression vectors, we used a modified pET21a vector with an N-terminal MBP tag. The coding sequences of *FKBP15-2*, *FKBP15-2^{D93A}*, *PcAvr3a12*, and *PcAvr3a14* without secretion and ER retention SP-encoding sequences were inserted into previously modified pET21a-MBP at the *EcoRI* and *XhoI* sites. All of these vectors were verified by sequencing. All of the previously used primers are listed in Supplemental Table 1.

Plant Materials and Growth Conditions

The *FKBP15-2* T-DNA insertion line (SALK_113542) was obtained from the ABRC. Homozygosity of T-DNA insertion mutants was confirmed by PCR using primers FP (GAT TAT GGC GAG CAA GAT GAG), RP (ATC CCT CAT CAT CTT CAT CCC), and BL1 (TGG TTC ACG TAG TGG GCC ATC G). All transgenic *A. thaliana* lines were generated by the floral dip method (Zhang et al., 2006) and screened on half-strength Murashige and Skoog (1/2 MS) plates with the appropriate antibiotics. Plant growing conditions for *A. thaliana* and *N. benthamiana* were the same as previously described (Pan et al., 2016).

Yeast Two-Hybrid Assay

The Y2H library screening and Y2H assays were performed using the Matchmaker Two-Hybrid System 3 protocol (Clontech). For screening of the Y2H library, the pGBKT7 vector containing the effector gene, acting as a bait, was transformed into yeast strain Y187. Positive yeast clones were mated with AH109 containing cDNA from *P. parasitica*-infected *A. thaliana* tissue, and the diploids were plated on SD/-Trp-Leu-His-Ade medium. We picked colonies from SD/-Trp-Leu-His-Ade medium and verified their sequence. For the Y2H assay, pGBKT7 and pGADT7 vectors, each containing a selection gene, were co-transformed into the yeast strain AH109. Transformations were verified by plating on SD/-Trp-Leu medium and interactions were confirmed based on growth on SD/-Trp-Leu-His medium containing 2.5 mM 3-amino-1,2,4-triazole (3AT), gain of β -galactosidase activity (β -gal), or growth on SD/-Trp-Leu-His-Ade medium.

Agroinfiltration and Confocal Laser Scanning Microscopy

Agrobacterium tumefaciens strain (GV3101) transformed with vector constructs was grown at 28°C for about 36 h in Luria–Bertani medium with appropriate antibiotics. *Agrobacterium* were pelleted, resuspended in infiltration buffer (10 mM MES, 10 mM MgCl₂, and 200 μ M acetosyringone), adjusted to the required concentration (OD₆₀₀ approximately 0.1–0.3), and infiltrated into 4- to 6-week-old *N. benthamiana* leaves.

Confocal images of infiltrated *N. benthamiana* leaves and stable transgenic *A. thaliana* leaves were taken using an Olympus IX83 confocal microscope (Japan). GFP and Venus expression was detected after excitation with a 488-nm wavelength laser, and emissions were collected between 500 and 540 nm. The fluorescence of mCherry was excited with a 559-nm wavelength laser to detect specific emissions between 600 and 680 nm.

Co-immunoprecipitation Assays

Three days after agroinfiltration, *N. benthamiana* leaves were detached and ground under liquid nitrogen with a mortar and pestle. Proteins were extracted with GTEN lysis buffer (10% glycerol, 25 mM Tris [pH 7.5], 1 mM EDTA, 150 mM NaCl) supplemented with 2% (w/v)

Molecular Plant

PVPP, 10 mM DTT, 1× protease inhibitor cocktail (Sigma), and 0.1% Tween 20 (Sigma), and precipitated by GFP-Trap agarose beads (Chromotek) or Anti-FLAG M2 affinity gel (Sigma) as described by Win et al. (2011). Precipitates were washed at least five times with GTEN buffer supplemented with 0.1% Tween 20. Fusion proteins from crude extracts (input) and precipitated proteins were detected by immunoblotting with protein-specific antibodies.

Protein Immunoblot Assays

Proteins were separated by SDS-PAGE and transferred from the gel to a PVDF membrane (Roche) in transfer buffer (25 mM Tris, 200 mM glycine, and 20% methanol). The membrane was then blocked in TBST buffer (Tris-buffered saline with 0.05% Tween 20 [pH 7.2]) containing 10% non-fat dry milk under gentle shaking. The blocked membrane was incubated with specific antibodies dissolved in TBSTM (TBST with 5% non-fat dry milk) at a ratio of 1:2000 and incubated at 4°C with shaking at 50 rpm overnight, followed by three washes (10 min each) with TBST. Next, the membrane was incubated with a secondary antibody coupled with horseradish peroxidase (HRP), which was also dissolved in TBSTM at a ratio of 1:2000, at room temperature for 1.5 h with shaking. Thereafter the membrane was washed three times (10 min each) with TBST and one time with TBS, then incubated with ECL (#CW0049S, ComWin) before photographing using a molecular imager (Chemidoc XRS+, Bio-Rad). The primary antibodies used in our experiments include anti-FLAG (#AE005, ABclonal), anti-GFP (#AE012, ABclonal), anti-myc (#AE010, ABclonal), and anti-HA (#HT301-01, Transgen). The secondary antibodies include HRP goat anti-mouse immunoglobulin G (IgG) (H + L) antibody (#AS013, ABclonal) and HRP goat anti-rabbit IgG (H + L) antibody (#AS014, ABclonal).

P. parasitica and *P. capsici* Culture Conditions and Inoculation Assays

The culture and zoospore production of *P. parasitica* and *P. capsici* were conducted as previously reported (Wang et al., 2011, 2013). The culture medium used for both *P. parasitica* and *P. capsici* was 5% (v/v) cleared carrot juice (CA) medium containing 0.002% (w/v) α -sitosterol and 0.01% (w/v) CaCO₃. The *P. capsici* strain used in this study was LT263, while the *P. parasitica* strain was Pp016.

For *P. capsici* inoculation assays, the abaxial surface of detached *A. thaliana* leaves was inoculated with a 10- μ l droplet containing ~80 *P. capsici* zoospores/ μ l. At 60 hpi, leaf discs (diameter 1 cm) around the zoospore droplets were collected with a puncher from at least eight leaves for one sample in each line. Genomic DNA was extracted using the CTAB method, and the pathogen biomass was quantified by real-time PCR as previously reported (Llorente et al., 2010). The results represented the ratio between pathogen and plant genomic DNA, and statistical significance was determined by one-way ANOVA followed by Tukey's multiple comparison test. The *P. parasitica* inoculation assays were performed similarly as those described above except that each leaf was wounded by toothpicks and wound sites were inoculated with a 10- μ l droplet with 200 *P. parasitica* zoospores/ μ l. *P. parasitica*-infected leaf discs were collected at 72 hpi. For *P. parasitica* root inoculation, roots of 14-day-old seedlings were dipped into a zoospore suspension (200 spores/ μ l) for 10 s and transferred to Petri dishes containing 1/2 MS medium without sugar. The root tissues of about 24 seedlings were pooled together for one sample. Pathogen biomass was quantified by RT-PCR as described above. All primers used can be found in Supplemental Table 2. The data diagrams were drawn by OriginPro.

Gene Expression Analyses

Total RNA was extracted using TRIzol (Invitrogen) reagent. For real-time qRT-PCR, cDNA was synthesized from 800 ng of total RNA using the PrimeScript RT Reagent Kit (TaKaRa). The qRT-PCR reactions were performed using the SYBR Premix Kit (Roche) according to manufacturers' instructions with 5- μ l template from a 1:20 dilution of cDNA. The primers we used are listed in Supplemental Table 2. The Ct values of genes were quantified using an iQ7 Real-Time Cycler (Life Tech-

PcAvr3a12 Targets and Inhibits a Plant PPIase

nologies, USA). Expression fold changes were calculated using the 2^{- $\Delta\Delta$ Ct} method. Statistical significance was determined by one-way ANOVA followed by Tukey's multiple comparison test. The data diagrams were drawn by OriginPro.

Recombinant Protein Expression and Purification

Constructs for production of recombinant MBP-GFP, MBP-PcAvr3a12, MBP-PcAvr3a14, MBP-FKBP15-2, and MBP-FKBP15-2^{D93A} proteins were introduced into *E. coli* strain BL21 (DE3). Cultures were incubated for 8 h with 0.4 mM isopropyl β -D-1-thiogalactopyranoside at 25°C–28°C with shaking at 180 rpm after cells grown at 37°C reached an OD₆₀₀ of 0.5–0.6. Cells were pelleted and resuspended with ice-cold lysis buffer (20 mM HEPES, 5 mM α -mercaptoethanol, 1 mM EDTA, 150 mM NaCl [pH 7.5]) containing 1× cocktail (Sigma). The resuspended cells were sonicated and centrifuged at 20,000 g for 30 min at 4°C. Crude proteins were affinity purified by amylose affinity chromatography (NEB), and the amylose resin column was washed with wash buffer (20 mM HEPES, 5 mM α -mercaptoethanol, 1 mM EDTA, 150 mM NaCl). Fusion proteins were eluted with wash buffer containing 10 mM maltose and were concentrated by centrifugation through an ultrafiltration tube (Merck). After purification, the purity of proteins was determined by SDS-PAGE and immunoblotting.

Rotamase (PPIase) Activity Assays

The rotamase activity of the recombinant FKBP15-2 and FKBP15-2^{D93A} proteins was determined through chymotrypsin-coupled assays (Harding et al., 1989). The purified recombinant proteins in assay buffer (40 mM HEPES, 0.015% Triton X-100, 150 mM NaCl [pH 7.9]) were mixed with 37.5 μ l of 5.6 nM succinyl-Ala-Leu-Pro-Phe-paranitroanilide (#S8511, Sigma), to generate a 2910- μ l mixture. This mixture was transferred into a cuvette before being placed in a UV-Vis spectrophotometer at 8°C. Each sample was pre-cooled at 8°C before measurement. The reactions were initiated by adding 90 μ l of 50 mg/ml chymotrypsin (#C3142, Sigma) and monitored by measuring absorbance at 390 nm every second for 5 min. Rapamycin, an inhibitor of PPIases, was obtained from Sigma (#V900930).

ACCESSION NUMBERS

Sequence data from this article can be found in the Arabidopsis Genome Data Library (<http://www.arabidopsis.org/>), Genome Bank Data Library (<https://www.ncbi.nlm.nih.gov/>), or *P. capsici* Genome Data Library (<https://genome.jgi.doe.gov/Phyca11/Phyca11.home.html>). Accession numbers: At3g25220, AtFKBP15-1; At5g48580, AtFKBP15-2; PITG_14371, PiAvr3a^{K1}; jgi|Phyca11|114071, PcAvr3a12; jgi|Phyca11|113768, PcAvr3a14; jgi|Phyca11|510076, PcFKBP35.

SUPPLEMENTAL INFORMATION

Supplemental Information is available at *Molecular Plant Online*.

FUNDING

This work was supported by the China Agriculture Research System (CARS-09), the National Natural Science Foundation of China (31125022 and 31561143007), and the Program of Introducing Talents of Innovative Discipline to Universities (Project 111) from the State Administration of Foreign Experts Affairs (#B18042).

AUTHOR CONTRIBUTIONS

W.S. and G.F. conceived and designed the experiments. G.F., Y.Y., W.L., T.L., and Q.W. performed the experiments. T.L. screened the Y2H library. G.F., X.Q., and W.S. analyzed the data. G.F., Y.D., X.Q., and W.S. wrote the manuscript. All authors reviewed the manuscript.

ACKNOWLEDGMENTS

We thank Dr. Brett Tyler (Oregon State University, USA), Dr. Patrick Schäfer (University of Warwick, UK), and Dr. Mingbo Wang (CSIRO

Agriculture, Canberra, Australia) for their insightful suggestions, Dr. Gary Loake (University of Edinburgh, UK) for advice on the PPIase activity assays, Xuguang Xi (Northwest A&F University, China) for providing the modified pET21a-MBP plasmid and assistance in protein purification, and Brett Tyler and Patrick Schäfer for manuscript editing. No conflict of interest declared. No conflict of interest declared.

Received: November 13, 2017

Revised: May 25, 2018

Accepted: May 27, 2018

Published: June 1, 2018

REFERENCES

- Attard, A., Gourgues, M., Callemeyn-Torre, N., and Keller, H.** (2010). The immediate activation of defense responses in *Arabidopsis* roots is not sufficient to prevent *Phytophthora parasitica* infection. *New Phytol.* **187**:449–460.
- Bertolotti, A., Zhang, Y., Hendershot, L.M., Harding, H.P., and Ron, D.** (2000). Dynamic interaction of BiP and ER stress transducers in the unfolded-protein response. *Nat. Cell Biol.* **2**:326–332.
- Boevink, P.C., Wang, X., McLellan, H., He, Q., Naqvi, S., Armstrong, M.R., Zhang, W., Hein, I., Gilroy, E.M., Tian, Z., et al.** (2016). A *Phytophthora infestans* RXLR effector targets plant PP1c isoforms that promote late blight disease. *Nat. Commun.* **7**:10311.
- Bos, J.I.B.** (2007). Function, structure and evolution of the RXLR effector AVR3a of *Phytophthora infestans*. PhD thesis (The Ohio State University).
- Bos, J.I.B., Armstrong, M.R., Gilroy, E.M., Boevink, P.C., Hein, I., Taylor, R.M., Zhendong, T., Engelhardt, S., Vetukuri, R.R., Harrower, B., et al.** (2010). *Phytophthora infestans* effector AVR3a is essential for virulence and manipulates plant immunity by stabilizing host E3 ligase CMPG1. *Proc. Natl. Acad. Sci. USA* **107**:9909–9914.
- Bozkurt, T.O., Schornack, S., Win, J., Shindo, T., Ilyas, M., Oliva, R., Cano, L.M., Jones, A.M.E., Huitema, E., Hoorn, R.A.L.V.D., et al.** (2011). *Phytophthora infestans* effector AVRblb2 prevents secretion of a plant immune protease at the haustorial interface. *Proc. Natl. Acad. Sci. USA* **108**:20832–20837.
- Bozkurt, T.O., Belhaj, K., Dagdas, Y.F., Chaparro-Garcia, A., Wu, C.H., Cano, L.M., and Kamoun, S.** (2015). Rerouting of plant late endocytic trafficking toward a pathogen interface. *Traffic* **16**:204–226.
- Braakman, I., and Hebert, D.N.** (2013). Protein folding in the endoplasmic reticulum. *Cold Spring Harb. Perspect. Biol.* **5**:a013201.
- Brandts, J.F., Brennan, M., and Lung-Nan, L.** (1977). Unfolding and refolding occur much faster for a proline-free proteins than for most proline-containing proteins. *Proc. Natl. Acad. Sci. USA* **74**:4178–4181.
- Chaparro-Garcia, A., Schwizer, S., Sklenar, J., Yoshida, K., Petre, B., Bos, J.I.B., Schornack, S., Jones, A.M.E., Bozkurt, T.O., and Kamoun, S.** (2015). *Phytophthora infestans* RXLR-WY effector AVR3a associates with Dynamin-Related Protein 2 required for endocytosis of the plant pattern recognition receptor FLS2. *PLoS One* **10**:e0137071.
- Coaker, G., Falick, A., and Staskawicz, B.** (2005). Activation of a phytopathogenic bacterial effector protein by a eukaryotic cyclophilin. *Science* **308**:548–550.
- Curtis, M.D., and Grossniklaus, U.** (2003). A gateway cloning vector set for high-throughput functional analysis of genes in planta. *Plant Physiol.* **133**:462–469.
- Dagdas, Y.F., Belhaj, K., Maqbool, A., Chaparro-Garcia, A., Pandey, P., Petre, B., Tabassum, N., Cruz-Mireles, N., Hughes, R., Sklenar, J., et al.** (2016). An effector of the Irish potato famine pathogen antagonizes a host autophagy cargo receptor. *Elife* **5**:e10856.
- Dodds, P.N., and Rathjen, J.P.** (2010). Plant immunity: towards an integrated view of plant-pathogen interactions. *Nat. Rev. Genet.* **11**:539–548.
- Dou, D., Kale, S.D., Wang, X., Chen, Y., Wang, Q., Wang, X., Jiang, R.H.Y., Arredondo, F.D., Anderson, R.G., Thakur, P.B., et al.** (2008). Conserved C-terminal motifs required for avirulence and suppression of cell death by *Phytophthora sojae* effector Avr1b. *Plant Cell* **20**:1118–1133.
- Dou, D., and Zhou, J.M.** (2012). *Phytopathogen* effectors subverting host immunity: different foes, similar battleground. *Cell Host Microbe* **12**:484–495.
- Du, Y., Mpina, M.H., Birch, P.R.J., Bouwmeester, K., and Govers, F.** (2015). *Phytophthora infestans* RXLR effector AVR1 interacts with exocyst component Sec5 to manipulate plant immunity. *Plant Physiol.* **169**:1975–1990.
- Gehl, C., Waadt, R., Kudla, J., Mendel, R.R., and Hänsch, R.** (2009). New GATEWAY vectors for high throughput analyses of protein-protein interactions by bimolecular fluorescence complementation. *Mol. Plant* **2**:1051–1058.
- Gilroy, E.M., Taylor, R.M., Hein, I., Boevink, P., Sadanandom, A., and Birch, P.R.J.** (2011). CMPG1-dependent cell death follows perception of diverse pathogen elicitors at the host plasma membrane and is suppressed by *Phytophthora infestans* RXLR effector AVR3a. *New Phytol.* **190**:653–666.
- Gleave, A.P.** (1992). A versatile binary vector system with a T-DNA organisational structure conducive to efficient integration of cloned DNA into the plant genome. *Plant Mol. Biol.* **20**:1203–1207.
- Haas, B.J., Kamoun, S., Zody, M.C., Jiang, R.H.Y., Handsaker, R.E., Cano, L.M., Grabherr, M., Kodira, C.D., Raffaele, S., Torto-Alalibo, T., et al.** (2009). Genome sequence and analysis of the Irish potato famine pathogen *Phytophthora infestans*. *Nature* **461**:393–398.
- Harding, M.W., Galat, A., Uehling, D.E., and Schreiber, S.L.** (1989). A receptor for the immunosuppressant FK506 is a *cis-trans* peptidyl-prolyl isomerase. *Nature* **341**:758–760.
- Harrar, Y., Bellini, C., and Faure, J.-D.** (2001). FKBP: at the crossroads of folding and transduction. *Trends Plant Sci.* **6**:426–431.
- Hausbeck, M.K., and Lamour, K.H.** (2004). *Phytophthora capsici* on vegetable crops: research progress and management challenges. *Plant Dis.* **88**:1292–1303.
- He, Z., Li, L., and Luan, S.** (2004). Immunophilins and parvulins: superfamily of peptidyl prolyl isomerases in *Arabidopsis*. *Plant Physiol.* **134**:1248–1267.
- Howell, S.H.** (2013). Endoplasmic reticulum stress responses in plants. *Annu. Rev. Plant Biol.* **64**:477–499.
- Jansen, G., Määttänen, P., Denisov, A.Y., Scarffe, L., Schade, B., Balghi, H., Dejgaard, K., Chen, L.Y., Muller, W.J., Gehring, K., et al.** (2012). An interaction map of endoplasmic reticulum chaperones and foldases. *Mol. Cell. Proteomics* **11**:710–723.
- Jiang, R.H.Y., Tripathy, S., Govers, F., and Tyler, B.M.** (2008). RXLR effector reservoir in two *Phytophthora* species is dominated by a single rapidly evolving superfamily with more than 700 members. *Proc. Natl. Acad. Sci. USA* **105**:4874–4879.
- Jing, M., Guo, B., Li, H., Yang, B., Wang, H., Kong, G., Zhao, Y., Xu, H., Wang, Y., Ye, W., et al.** (2016). A *Phytophthora sojae* effector suppresses endoplasmic reticulum stress-mediated immunity by stabilizing plant binding immunoglobulin proteins. *Nat. Commun.* **7**:11685.
- Jones, J.D., and Dangl, J.L.** (2006). The plant immune system. *Nature* **444**:323–329.
- Kale, S.D., Gu, B., Capelluto, D.G.S., Dou, D., Feldman, E., Rumore, A., Arredondo, F.D., Hanlon, R., Fudal, I., Rouxel, T., et al.** (2010).

- External lipid PI3P mediates entry of eukaryotic pathogen effectors into plant and animal host cells. *Cell* **142**:284–295.
- Kamoun, S., Furzer, O., Jones, J.D.G., Judelson, H.S., Ali, G.S., Dalio, R.J.D., Roy, S.G., Schena, L., Zambounis, A., Panabières, F., et al.** (2015). The top 10 oomycete pathogens in molecular plant pathology. *Mol. Plant Pathol.* **16**:413–434.
- Kazan, K., and Lyons, R.** (2014). Intervention of phytohormone pathways by pathogen effectors. *Plant Cell* **26**:2285–2309.
- Körner, C., Du, X., Vollmer, M., and Pajeroska-Mukhtar, K.** (2015). Endoplasmic reticulum stress signaling in plant immunity—at the crossroad of life and death. *Int. J. Mol. Sci.* **16**:25964.
- Kong, G., Zhao, Y., Jing, M., Huang, J., Yang, J., Xia, Y., Kong, L., Ye, W., Xiong, Q., Qiao, Y., et al.** (2015). The activation of *phytophthora* effector Avr3b by plant cyclophilin is required for the nudix hydrolase activity of Avr3b. *PLoS Pathog.* **11**:e1005139.
- King, S.R.F., McLellan, H., Boevink, P.C., Armstrong, M.R., Bukharova, T., Sukarta, O., Win, J., Kamoun, S., Birch, P.R.J., and Banfield, M.J.** (2014). *Phytophthora infestans* RXLR effector PexRD2 interacts with host MAPKKK α to suppress plant immune signaling. *Plant Cell* **26**:1345–1359.
- Lamour, K.H., Mudge, J., Gobena, D., Hurtado-Gonzales, O.P., Schmutz, J., Kuo, A., Miller, N.A., Rice, B.J., Raffaele, S., Cano, L.M., et al.** (2012). Genome sequencing and mapping reveal loss of heterozygosity as a mechanism for rapid adaptation in the vegetable pathogen *Phytophthora capsici*. *Mol. Plant Microbe Interact.* **25**:1350–1360.
- Lang, K., Schmid, F.X., and Fischer, G.** (1987). Catalysis of protein folding by prolyl isomerase. *Nature* **329**:268–270.
- Li, J., Zhao-Hui, C., Batoux, M., Nekrasov, V., Roux, M., Chinchilla, D., Zipfel, C., and Jones, J.D.** (2009). Specific ER quality control components required for biogenesis of the plant innate immune receptor EFR. *Proc. Natl. Acad. Sci. USA* **106**:15973–15978.
- Liu, J.X., and Howell, S.H.** (2010). Endoplasmic reticulum protein quality control and its relationship to environmental stress responses in plants. *Plant Cell* **22**:2930–2942.
- Llorente, B., Bravo-Almonacid, F., Cvitanich, C., Orlowska, E., Torres, H.N., Flawia, M.M., and Alonso, G.D.** (2010). A quantitative real-time PCR method for in planta monitoring of *Phytophthora infestans* growth. *Let. Appl. Microbiol.* **51**:603–610.
- Luan, S., Kudla, J., Gruissem, W., and Schreiber, S.L.** (1996). Molecular characterization of a FKBP-type immunophilin from higher plants. *Proc. Natl. Acad. Sci. USA* **93**:6964–6969.
- Lucke, C., and Weiwad, M.** (2011). Insights into immunophilin structure and function. *Curr. Med. Chem.* **18**:5333–5354.
- McLellan, H., Boevink, P.C., Armstrong, M.R., Pritchard, L., Gomez, S., Morales, J., Whisson, S.C., Beynon, J.L., and Birch, P.R.J.** (2013). An RxLR Effector from *Phytophthora infestans* prevents re-localisation of two plant NAC transcription factors from the endoplasmic reticulum to the nucleus. *PLoS Pathog.* **9**:e1003670.
- Moreno, A.A., Mukhtar, M.S., Blanco, F., Boatwright, J.L., Moreno, I., Jordan, M.R., Chen, Y., Brandizzi, F., Dong, X., Orellana, A., et al.** (2012). IRE1/bZIP60-mediated unfolded protein response plays distinct roles in plant immunity and abiotic stress responses. *PLoS One* **7**:e31944.
- Nelson, B.K., Cai, X., and Nebenfuhr, A.** (2007). A multicolored set of in vivo organelle markers for co-localization studies in *Arabidopsis* and other plants. *Plant J.* **51**:1126–1136.
- Nekrasov, V., Li, J., Batoux, M., Roux, M., Chu, Z.H., Lacombe, S., Rougon, A., Bittel, P., Kiss-Papp, M., Chinchilla, D., et al.** (2009). Control of the pattern-recognition receptor EFR by an ER protein complex in plant immunity. *EMBO J.* **28**:3428–3438.
- Pan, Q., Cui, B., Deng, F., Quan, J., Loake, G.J., and Shan, W.** (2016). *RTP1* encodes a novel endoplasmic reticulum (ER)-localized protein in *Arabidopsis* and negatively regulates resistance against biotrophic pathogens. *New Phytol.* **209**:1641–1654.
- Partaledis, J.A., and Berlin, V.** (1993). The FKBP2 gene of *Saccharomyces cerevisiae*, encoding the immunosuppressant-binding protein FKBP-13, is regulated in response to accumulation of unfolded proteins in the endoplasmic reticulum. *Proc. Natl. Acad. Sci. USA* **90**:5450–5454.
- Pogorelko, G.V., Mokryakova, M., Fursova, O.V., Abdeeva, I., Piruzian, E.S., and Bruskin, S.A.** (2014). Characterization of three *Arabidopsis thaliana* immunophilin genes involved in the plant defense response against *Pseudomonas syringae*. *Gene* **538**:12–22.
- Qiang, X., Zechmann, B., Reitz, M.U., Kogel, K.-H., and Schäfer, P.** (2012). The mutualistic fungus *piriformospora indica* colonizes *Arabidopsis* roots by inducing an endoplasmic reticulum stress-triggered caspase-dependent cell death. *Plant Cell* **24**:794–809.
- Qiao, Y., Liu, L., Xiong, Q., Flores, C., Wong, J., Shi, J., Wang, X., Liu, X., Xiang, Q., Jiang, S., et al.** (2013). Oomycete pathogens encode RNA silencing suppressors. *Nat. Genet.* **45**:330–333.
- Qiao, Y., Shi, J., Zhai, Y., Hou, Y., and Ma, W.** (2015). *Phytophthora* effector targets a novel component of small RNA pathway in plants to promote infection. *Proc. Natl. Acad. Sci. USA* **112**:5850–5855.
- Rehmany, A.P., Gordon, A., Rose, L.E., Allen, R.L., Armstrong, M.R., Whisson, S.C., Kamoun, S., Tyler, B.M., Birch, P.R.J., and Beynon, J.L.** (2005). Differential recognition of highly divergent downy mildew avirulence gene alleles by *RPP1* resistance genes from two *Arabidopsis* lines. *Plant Cell* **17**:1839–1850.
- Romano, P., Gray, J., Horton, P., and Luan, S.** (2005). Plant immunophilins: functional versatility beyond protein maturation. *New Phytol.* **166**:753–769.
- Shan, W.X., Cao, M., Leung, D., and Tyler, B.M.** (2004). The Avr1b locus of *Phytophthora sojae* encodes an elicitor and a regulator required for avirulence on soybean plants carrying resistance gene Rps1b. *Mol. Plant Microbe Interact.* **17**:394–403.
- Turnbull, D., Yang, L., Naqvi, S., Breen, S., Welsh, L., Stephens, J., Morris, J., Boevink, P.C., Hedley, P.E., Zhan, J., et al.** (2017). RXLR effector AVR2 up-regulates a brassinosteroid responsive bHLH transcription factor to suppress immunity. *Plant Physiol.* **174**:356–369.
- Tyler, B.M., Tripathy, S., Zhang, X., Dehal, P., Jiang, R.H., Aerts, A., Arredondo, F.D., Baxter, L., Bensasson, D., Beynon, J.L., et al.** (2006). *Phytophthora* genome sequences uncover evolutionary origins and mechanisms of pathogenesis. *Science* **313**:1261–1266.
- Uknes, S., Dincher, S., Friedrich, L., Negrotto, D., Williams, S., Thompson-taylor, H., Potter, S., Ward, E., and Ryals, J.** (1993). Regulation of pathogenesis-related protein-1a gene-expression in tobacco. *Plant Cell* **5**:159–169.
- Vasudevan, D., Gopalan, G., Kumar, A., Garcia, V.J., Luan, S., and Swaminathan, K.** (2015). Plant immunophilins: a review of their structure-function relationship. *Biochim. Biophys. Acta* **1850**:2145–2158.
- Vega-Arreguin, J.C., Jalloh, A.S., Bos, J.I.B., and Moffett, P.** (2014). Recognition of an Avr3a homologue plays a major role in mediating nonhost resistance to *Phytophthora capsici* in *Nicotiana* species. *Mol. Plant Microbe Interact.* **27**:770–780.
- Wakasa, Y., Oono, Y., Yazawa, T., Hayashi, S., Ozawa, K., Handa, H., Matsumoto, T., and Takaiwa, F.** (2014). RNA sequencing-mediated transcriptome analysis of rice plants in endoplasmic reticulum stress conditions. *BMC Plant Biol.* **14**:101.
- Wang, D., Weaver, N.D., Kesarwani, M., and Dong, X.** (2005). Induction of protein secretory pathway is required for systemic acquired resistance. *Science* **308**:1036–1040.

- Wang, Y., Meng, Y., Zhang, M., Tong, X., Wang, Q., Sun, Y., Quan, J., Govers, F., and Shan, W. (2011). Infection of *Arabidopsis thaliana* by *Phytophthora parasitica* and identification of variation in host specificity. *Mol. Plant Pathol.* **12**:187–201.
- Wang, Y., Bouwmeester, K., Mortel, J.E.V.D., Shan, W., and Govers, F. (2013). A novel *Arabidopsis*-oomycete pathosystem: differential interactions with *Phytophthora capsici* reveal a role for camalexin, indole glucosinolates and salicylic acid in defence. *Plant Cell Environ.* **36**:1192–1203.
- Wang, X., Boevink, P., McLellan, H., Armstrong, M., Bukharova, T., Qin, Z., and Birch, P.R.J. (2015). A host KH RNA-binding protein is a susceptibility factor targeted by an RXLR effector to promote late blight disease. *Mol. Plant* **8**:1385–1395.
- Wang, S., Boevink, P.C., Welsh, L., Zhang, R., Whisson, S.C., and Birch, P.R.J. (2017). Delivery of cytoplasmic and apoplastic effectors from *Phytophthora infestans* haustoria by distinct secretion pathways. *New Phytol.* **216**:205–215.
- Wawra, S., Trusch, F., Matena, A., Apostolakis, K., Linne, U., Zhukov, I., Stanek, J., Kořmiňski, W., Davidson, I., Secombes, C., et al. (2017). The RxLR motif of the host targeting effector AVR3a of *Phytophthora infestans* is cleaved before secretion. *Plant Cell* **29**:1184–1195.
- Win, J., Kamoun, S., and Jones, A.E. (2011). Purification of effector-target protein complexes via transient expression in *Nicotiana benthamiana*. In *Plant Immunity*, J.M. McDowell, ed. (New York: Humana Press), pp. 181–194.
- Wesley, S.V., Helliwell, C.A., Smith, N.A., Wang, M., Rouse, D.T., Liu, Q., Gooding, P.S., Singh, S.P., Abbott, D., Stoutjesdijk, P.A., et al. (2001). Construct design for efficient, effective and high-throughput gene silencing in plants. *Plant J.* **27**:581–590.
- Whisson, S.C., Boevink, P.C., Moleleki, L., Avrova, A.O., Morales, J.G., Gilroy, E.M., Armstrong, M.R., Grouffaud, S., West, P.V., Chapman, S., et al. (2007). A translocation signal for delivery of oomycete effector proteins into host plant cells. *Nature* **450**:115–118.
- Yang, L., McLellan, H., Naqvi, S., He, Q., Boevink, P.C., Armstrong, M., Giuliani, L.M., Zhang, W., Tian, Z., Zhan, J., et al. (2016). Potato NPH3/RPT2-like protein StNRL1, targeted by a *Phytophthora infestans* RXLR effector, is a susceptibility factor. *Plant Physiol.* **171**:645–657.
- Yun, B.W., Atkinson, H.A., Gaborit, C., Greenland, A., Read, N.D., Pallas, J.A., and Loake, G.J. (2003). Loss of actin cytoskeletal function and EDS1 activity, in combination, severely compromises non-host resistance in *Arabidopsis* against wheat powdery mildew. *Plant J.* **34**:768–777.
- Zhang, X., Henriques, R., Lin, S.S., Niu, Q.W., and Chua, N.H. (2006). *Agrobacterium*-mediated transformation of *Arabidopsis thaliana* using the floral dip method. *Nat. Protoc.* **1**:641–646.